Feature Article

JCBFM

Journal of Cerebral Blood Flow & Metabolism
2017, Vol. 37(10) 3278–3299

DOI: 10.1177/0271678X17724681
journals.sagepub.com/home/jcbfm
SAGE

New astroglial injury-defined biomarkers for neurotrauma assessment

Julia Halford[1], Sean Shen[2], Kyohei Itamura[1], Jaclynn Levine[1], Albert C Chong[1], Gregg Czerwieniec[2], Thomas C Glenn[3], David A Hovda[3], Paul Vespa[4], Ross Bullock[5], W Dalton Dietrich[6], Stefania Mondello[7], Joseph A Loo[2,8] and Ina-Beate Wanner[1]

Abstract

Traumatic brain injury (TBI) is an expanding public health epidemic with pathophysiology that is difficult to diagnose and thus treat. TBI biomarkers should assess patients across severities and reveal pathophysiology, but currently, their kinetics and specificity are unclear. No single ideal TBI biomarker exists. We identified new candidates from a TBI CSF proteome by selecting trauma-released, astrocyte-enriched proteins including aldolase C (ALDOC), its 38kD breakdown product (BDP), brain lipid binding protein (BLBP), astrocytic phosphoprotein (PEA15), glutamine synthetase (GS) and new 18-25kD-GFAP-BDPs. Their levels increased over four orders of magnitude in severe TBI CSF. First post-injury week, ALDOC levels were markedly high and stable. Short-lived BLBP and PEA15 related to injury progression. ALDOC, BLBP and PEA15 appeared hyper-acutely and were similarly robust in severe and mild TBI blood; 25kD-GFAP-BDP appeared overnight after TBI and was rarely present after mild TBI. Using a human culture trauma model, we investigated biomarker kinetics. Wounded (mechanoporated) astrocytes released ALDOC, BLBP and PEA15 acutely. Delayed cell death corresponded with GFAP release and proteolysis into small GFAP-BDPs. Associating biomarkers with cellular injury stages produced astroglial injury-defined (AID) biomarkers that facilitate TBI assessment, as neurological deficits are rooted not only in death of CNS cells, but also in their functional compromise.

Keywords

Astrocytes, brain trauma, proteomics, cell culture, cerebrospinal fluid, exploratory factor analysis

Received 14 December 2016; Revised 1 May 2017; Accepted 25 May 2017

Introduction

Traumatic brain injury (TBI) is an expanding global public health concern and is the leading cause of death and disability among youth.[1] The TBI spectrum covers a wide range of severities with multiple adverse outcomes.[2] The most common TBIs are mild and occur frequently during sports activities and military operations. Some mild TBI patients develop persisting neurological deficits that would be desirable to predict.[3,4] Unambiguous diagnosis, both real-time and delayed, is paramount for safe return-to-action because

[1]Semel Institute for Neuroscience and Human Behavior, University of California, Los Angeles, CA, USA
[2]Department of Chemistry and Biochemistry, University of California, Los Angeles, CA, USA
[3]Department of Neurosurgery, Brain Injury Research Center, Department of Molecular and Medical Pharmacology
[4]Department of Neurology, UCLA-David Geffen School of Medicine, Los Angeles, CA, USA
[5]Department of Neurological Surgery, Jackson Memorial Hospital, Miami, FL, USA
[6]The Miami Project to Cure Paralysis, University of Miami-Miller School of Medicine, Miami, FL, USA
[7]Department of Biomedical and Dental Sciences and Morphofunctional Imaging, University of Messina, Messina, Italy
[8]Department of Biological Chemistry, UCLA Molecular Biology Institute, and UCLA/DOE Institute for Genomics and Proteomics, University of California, Los Angeles, CA, USA

Corresponding author:
Ina B Wanner, Semel Institute for Neuroscience and Human Behavior, UCLA, 635 Charles E Young Drive South, NRB 260, Los Angeles, CA 90095, USA.
Email: iwanner@mednet.ucla.edu

repeated head impacts can exacerbate symptoms and increase risk for later neurological deficits.[5]

TBI is heterogeneous with variable periods of coma, different pathologies such as intracranial hematoma, contusion or axonal injury and complex injury evolution.[6] Diagnosing TBI pathology is difficult, and monitoring progression is often impractical, confounding treatment of TBI patients. Further, clinical endpoints with variable degrees of brain dysfunction are hard to predict. Current clinical approaches to assessing TBI patients, based on the Glasgow Coma Scale (GCS) and computed tomography (CT)-scans, incompletely capture TBI complexity.[7] While CT-scans are common and report macroscopic brain lesions, detection of diffuse microstructural injuries and metabolic dysfunction after TBI requires more refined and advanced imaging techniques that are less accessible.[8,9] Microstructural injuries such as fiber damage and cell membrane permeability (mechanoporation) are accompanied by protein changes that can provide insight into early cellular and structural pathophysiology following TBI.[10–14] We hypothesize that cellular injury processes and their protein signatures are useful resources for improving the acute assessment of neurotrauma patients.

Many studies have been conducted to identify new neurotrauma protein biomarker candidates.[15,16] GFAP, neuron specific enolase, neurofilaments, tau, ubiquitin C-terminal hydrolase (UCHL1) and S100 β have been previously chosen for their neuropathological presence. While these candidates' expression in neurons or glia is well known, their trauma-induced release mechanisms are not well established. Furthermore, clinical translation of these candidate biomarkers is limited by their short-lived biofluid presence, extra-CNS sources, delayed circulatory appearance and age-dependent contingencies.[17,18] Most protein biomarker mining studies have drawbacks, including failure to address fluid changes, differences in time-scales between rodent and human pathophysiology and analytical challenges that obstruct the identification of new biomarkers.[19–22] Furthermore, selection of suitable biomarker candidates from untargeted (global) proteomics discovery experiments is difficult and often unsuccessful.[23] These observations emphasize the need for a new class of biomarkers associated directly and immediately with traumatic impact on brain cells.

Astrocytes were chosen as the study's focus due to their central roles in the neuro vascular unit including brain metabolism, blood flow and blood–brain barrier (BBB) function.[24–26] Astrocytes outnumber neurons in the human neocortical white matter and are vulnerable and responsive to injury.[13,27–29] We recently reported that substantial amounts of cellular proteins are released into fluids minutes after abrupt astrocyte stretch-injury.[30] Overall, astrocytes are ideal sources for neurotrauma biomarkers.

In the present work, we determined a TBI cerebrospinal fluid (CSF) proteome and a strategy to overcome the typical "proteomics bottlenecks." We capitalized on astrocyte enrichment and our previous work on initial trauma-released proteins to identify a panel of new neurotrauma biomarker candidates.[26,30–32] Clinical studies documented new biomarker elevation and new profiles in severe TBI patients' biofluids and explored early presence of these biomarkers in serum of mild TBI patients. Surprisingly, our parallel studies in a simple human culture trauma model produced similar profiles early post injury. We then linked the biomarker profiles with coinciding cell injury processes. Importantly, biomarkers of cell wounding and cell death provide biosignatures of brain cell compromise and demise. Thus, our new astroglial injury-defined (AID) biomarkers could become powerful tools for understanding TBI pathophysiology.

Materials and methods

Donors, patients, samples and ethics guidelines

This study follows UCLA Policy 991, which follows guidelines from the Belmont report and is enforced by the Office of Human Research Protection Program.[33] All CSF and plasma samples were collected under protocols approved by the Institutional Review Boards of UCLA-David Geffen School of Medicine, University of Miami-Miller School of Medicine and University of Messina. Written informed consent was obtained from patients or authorized representatives. CSF from TBI patients was collected by ventriculostomy, and blood by venipuncture as early as 1 h and up to every 6 h over a maximum of five days following injury. The inclusion criteria were a post-resuscitation GCS score of eight or less for severe TBI patients (GCS < 8) and larger than eight (GCS 9–12) for moderate TBI patients. Adult patients admitted to the emergency department with mild TBI (GCS 13 to 15) within 4 h after injury and requiring a CT as part of their initial management were also included. The exclusion criteria were no informed consent, patients younger than 16 years old, no head CT scan, pregnant women, prisoners or history of psychotic illness or neurological disease. CSF control samples were obtained by lumbar drain from patients with unruptured aneurysms (UCLA) or were donated from healthy subjects (Precision-Med). Subject details are listed in Supplementary Table 1. CSF, plasma and serum samples were handled following common data elements for biomarker studies and protocols have been approved by UCLA Institutional Biosafety Committee.[34]

CSF proteomics

Equal CSF volumes from TBI patients and healthy subjects were dried, reduced, alkylated and trypsin digested (for details, see Supplementary Methods). The resulting samples were acidified, cleared of precipitates and then dried. Protocol details are provided in Supplementary Methods. For mass spectrometry measurements, the CSF tryptic digests were reconstituted and desalted, and liquid chromatography-tandem mass spectrometry (LC-MS/MS) was conducted using an LTQ-Orbitrap or Q-Exactive Orbitrap mass spectrometer (Thermo Scientific). Peptide separation, acquisition, analysis and validation details are provided in Supplementary Methods.

Immunoblotting, sub-saturated densitometry and technical variance

Conditioned media of the human astroglial trauma model were collected from six cultures (12 ml); samples were prepared as described previously.[30] Clinical biofluid samples were treated following common data element recommendations.[34] Sample preparation details are given in Supplementary Methods. Immunoblotting was performed as described with details provided previously and in Supplementary Methods.[30] All fluid analyses were normalized by volume (30 µl/lane). Signal specificity was validated using different specific antibodies for GFAP and GS and isoform-specific antibodies for ALDOC and BLBP (Supplementary Table 2). His-tagged pure proteins ALDOC, BLBP, PEA15 (EnCor Biotechnology) and GFAP full size, 37 kD and 20 kD fragments (Abbott Diagnostics) were analyzed in parallel (Supplementary Table 3). Secondary antibodies are listed in Supplementary Table 4. Multiple films of different exposure lengths were applied consistently. Densitometry is described in detail in the Supplementary Methods and Supplementary Figure 1. Post hoc normalization within an expanded linear range covered two to four orders of magnitude. Overall, analysis variance was at least 10-fold smaller than significant cross-condition differences. In the trauma model, each biomarker's release varied no more than 1–2 z-scores.

Quantitation of biomarkers in CSF using multiple reaction monitoring-mass spectrometry

Internal standard peptides specific to each biomarker were synthesized with heavy isotope-labeled arginine and lysine and spiked into CSF samples (Thermo Scientific, see Supplementary Table 5). CSF samples were reduced, alkylated, and then digested before undergoing drying, reconstitution and desalting, as described in Supplementary Methods. Samples were analyzed using either a Q-Exactive Orbitrap MS or a 4000 QTRAP triple quadrupole MS (AB Sciex). Peptides were fragmented into their components by high-energy collision, and the resulting product ions were measured as transitions (Supplementary Table 5). Biomarker concentrations were calculated based on area under the curve. The signal levels from three transitions are summed for each biomarker and the signal ratio of the endogenous to the heavy labeled peptide was determined (see Supplementary Methods).

Human astroglial trauma model

Primary human astrocytes were prepared from donated, de-identified human fetal cerebral neocortices at 16–19 gestational weeks as described previously.[35] After mechanical dissociation, astrocytes were subsequently isolated by size in a 33% Percoll gradient (Sigma). Washed cells were cultured in T150 cell culture-treated plastic flasks (Corning). Purified astrocytes were seeded at a density of ~135,000 human cells/962 mm^2 onto collagen-coated deformable membranes (Bioflex, Flexcell Intl.; see Supplementary Methods for cell isolation, purification and passaging). Serum was stepwise removed, leading to expression of mature astrocyte morphology and markers as previously described.[35] Cultures were stretch-injured using one mild (2.6–4.0 psi) or severe (4.4–5.3 psi) 50 ms pressure-pulse produced by a CIC II pressure controller (custom design and fabrication).

Cell permeability and viability assays, immunocytochemistry and analyses

Cell death and permeability rates were determined in unstretched cultures and at various times after stretching for every donor. Dead cells had small nuclei with condensed chromatin (pyknotic) and took up propidium iodide (PI) due to integrity loss.[36] Integrity compromised, wounded cells had control-shaped nuclei with PI-stain due to transient plasma membrane permeability.[30] After fixation, all nuclei were stained using Hoechst. On average, 800 cells per culture were counted in randomly chosen images and all nuclei were scored as belonging to intact (PI-negative), leaky or dead cells. Percentages of dead and wounded cells were calculated and averages and standard deviations determined. Live-staining details are given in Supplementary Methods. PI-stained cultures were counter-stained for astroglial biomarkers using antibodies and procedures listed in Supplementary Methods. Cellular immunofluorescence intensities for BLBP, ALDOC and PEA15 were measured using ImageJ in 100–160 cells for each biomarker in control and 30 min post-stretch cultures for three to five donors. Single-cell

biomarker intensities after stretching were normalized to those of unstretched cells; means were plotted as percent of control. In addition, binary scoring produced percent cell populations with biomarker intensity decrease. On average, 500 cells for each biomarker were scored in four to seven cultures of each condition (control, 30 min post stretch). Pie charts were generated by grouping intact and leaky cells by PI-positivity. Then, the fraction of cells with decreased biomarker levels was determined in the two groups as previously described.[30] For assessment of acute post-injury biomarker status, the small percentage of dead cells was not included.

Statistical analyses

Quantitative analyses of clinical samples. Optical density (OD) measurements were log-transformed for normal distribution and standardized; analytical replicates were averaged. TBI patient biomarker levels were compared to controls and over time by factorial analysis of variance (ANOVA), assuming independence across time. Repeated measures (mixed model) ANOVA with non-constant intra-class variances over time yielded the same results. Immunoblot and MRM-MS measures correlated by Spearman rank and their strengths were evaluated using quantile–quantile plots. MRM-MS concentration differences across biomarkers were compared using repeated measures ANOVA mixed model with non-constant variance. Exploratory factor analysis (EFA) was carried out for all 10 biomarkers. A biomarker was retained as part of a factor if its loading exceeded 0.50. Factors were estimated using an iterative method of maximum likelihoods and a varimax rotation.[37,38] Classification tree analysis partitioned the cohort by determining factor thresholds for TBI survivors, nonsurvivors and controls.[39]

Quantitative analyses in the trauma model. Donor-paired log-transformed biomarker culture fluid levels were compared using repeated measures (mixed model) ANOVA with homogeneous variances over time.[40] Associations between biomarker levels and cell fate were quantified using Spearman correlation coefficients. Cell wounding and cell death mean differences were determined using mixed model ANOVA allowing for non-constant variance and random donor effects. Percent wounded and dead cells were normally distributed but had different standard deviations. Cell number-weighted means were used for all cell fate and biomarker scoring data and intensity measurements. Single-cell immunofluorescence densities were compared using Student's or Welch-corrected *t*-tests or Mann–Whitney U test. Statistical analyses were conducted using Sigmaplot, Excel, Instat (Graphpad), JMP and SAS (version 9.4).

Results

Cerebrospinal fluid of TBI patients carries a signature of trauma-released astroglial proteins

A proteomic approach identified proteins in CSF from 19 TBI patients and 9 control subjects. Among the 484 proteins identified, 232 were unique to TBI, while 252 overlapped with the control CSF proteome (Supplementary Figure S2, Supplementary Table 6). To select neurotrauma biomarker candidates, we determined the overlap with our previously published trauma-released proteins that were elevated in conditioned medium of cultured mouse astrocytes after stretch-injury[30] (Supplementary Figures S2 and S3). This comparison identified proteins released as direct consequence of mechanical trauma, 62% of which were represented in the human TBI CSF proteome. To further improve specificity, we determined astrocyte-enriched proteins using published gene array data and excluded proteins found in plasma from healthy individuals or are abundant outside the CNS.[31,41–44] From this, four astroglial injury-associated proteins were identified: (1) aldolase C (ALDOC), which is exceptional, both in astrocyte enrichment and abundance among brain proteins,[30,45] (2) glutamine synthetase (GS, also known as GLNA), (3) brain lipid binding protein (BLBP, also known as brain fatty acid binding protein, FABP7) and (4) astrocytic phosphoprotein 15 (PEA15). To assess their diagnostic value, we confirmed their presence and quantified amounts of these candidate biomarkers in TBI patient biofluids using two independent approaches: immunoblotting with scaled densitometry and multiple reaction monitoring-mass spectrometry (MRM-MS).

TBI patients show distinct AID biomarker profiles in CSF and blood across trauma severities

We analyzed CSF from 26 severe TBI patients and 13 control subjects (Figure 1). Supplementary Table 1 displays the characteristics of the controls (1A) and severe TBI patients (1B). Longitudinal samples were available from six TBI patients. The CSF levels of the new astroglial biomarkers, ALDOC, GS, BLBP and PEA15 were measured and compared with two previously studied ones, GFAP and S100β. Immunoblot data of the serum protein apolipoprotein B (APOB) in CSF indicated blood entry, as APOB was absent from control CSF (Supplementary Table 6). Use of APOB in this manner is independently supported by previous work in a rodent spinal cord injury CSF proteomic study.[15] The abundant CSF protein prostaglandin synthase (PTGDS) served as a CSF standard. Immunoblot signals for those eight proteins in CSF

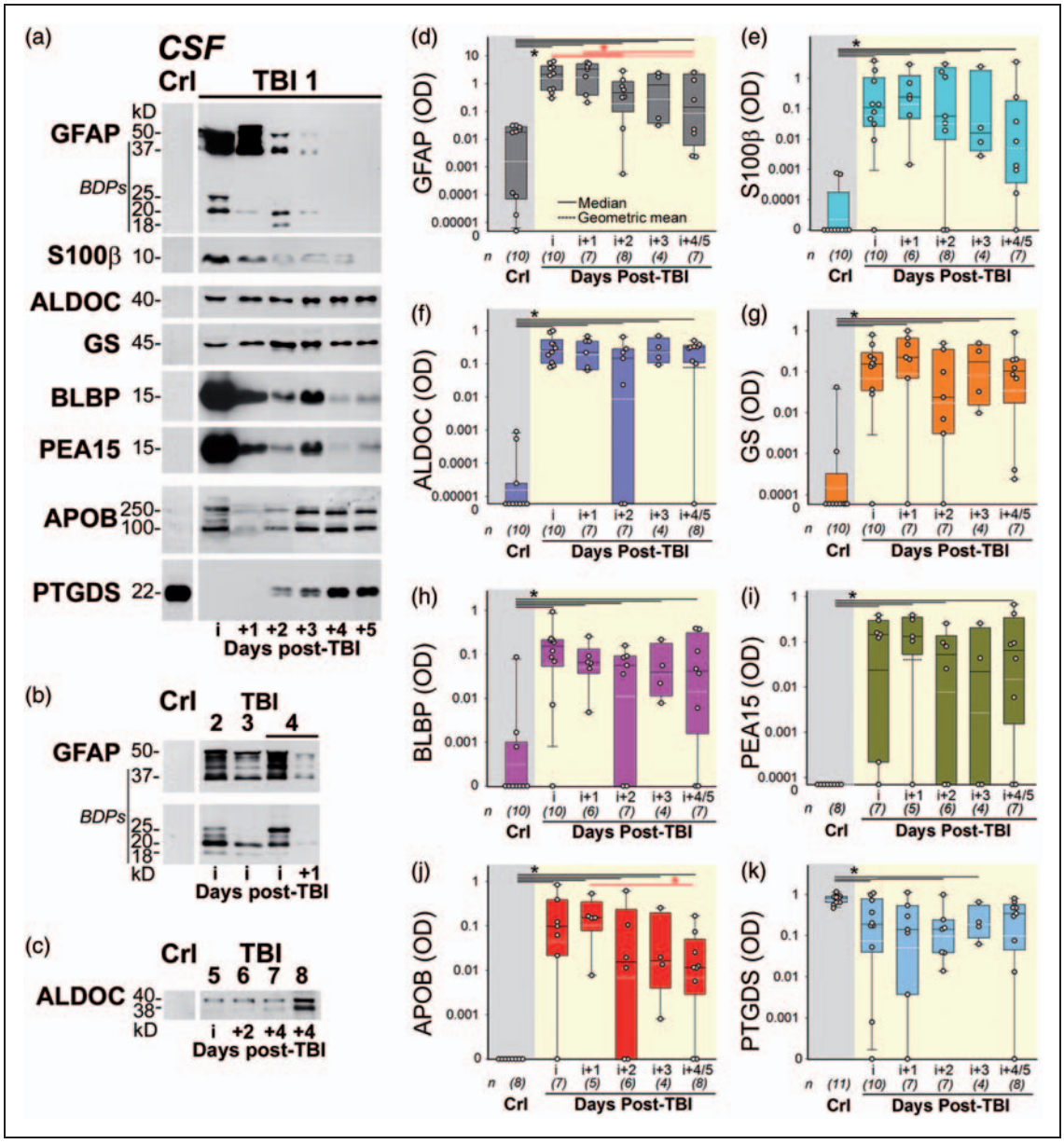

Figure 1. Biomarkers show diverse temporal CSF profiles during the first week after TBI. (a) Immunoblots of 30 μl CSF samples show GFAP (50 kD with BDPs 37, 25, 20 and 18 kD), S100 β (10 kD), ALDOC (40 kD), GS (45 kD), BLBP (15 kD) and PEA15 (15 kD) on injury day (i) and five post-injury days (i + 1 to i + 5) in a severe TBI patient (TBI 1, clinical data see Supplementary Table 1(b)). These data are shown alongside a control (Crl). Bleeding indicator APOB (130 + 250 kD) varied over time post injury and was absent in control. CSF standard PTGDS (22 kD) had robust signal in Crl but was absent immediately after TBI with slow recovery. (b) CSF samples (30 μl/lane) from three TBI patients (TBI 2 to 4) showed variable GFAP levels, exhibiting full size signal in addition to both large breakdown products (50–37 kD BDPs) and small BDPs (25 kD, 20 + 18 kD) on injury day and day i + 1. Control lacked GFAP signal. (c) CSF immunoblots (30 μl/lane) show full size ALDOC in four TBI patients (TBI 5 to 8) and variable intensity of a 38 kD ALDOC-BDP on i + 4 in two patients (TBI 7, 8). Control lacked ALDOC signal. (d–k) Box-and-whisker plots show median (black line) and geometric means (white dashed line) of exposure-normalized CSF immunoblot optical densities (OD) of astroglial biomarkers, APOB and PTGDS from 20–25 TBI patients (on injury day to day i + 5) and 8–11 Controls. Individual data points are shown, and data shown on a log-spaced axis. Data from post-injury days 4 and 5 were combined, as values did not differ significantly (repeated measures mixed ANOVA). n = subject numbers listed for each day, and same day replicates were averaged. See Supplementary Methods for quantification. (d) Total GFAP was elevated on all TBI days (*$p < 0.05$) but declined over indicated times (red asterisk, *$p < 0.002$). (e) S100 β levels were higher on all TBI days versus controls (*$p < 0.0022$). (f) ALDOC ($p < 0.004$) and (g) GS ($p < 0.001$) were elevated on all TBI days without significant decline over time. (h) BLBP ($p < 0.03$) and (i) PEA15 ($p < 0.004$) were elevated after TBI on indicated days. (j) APOB was elevated in TBI versus Crl (*$p < 0.005$). (k) PTGDS decreased variably on indicated TBI days versus Crl (*$p < 0.004$), with mean PTGDS level recovering four to five days post TBI.

showed different temporal profiles in one severe TBI patient during the first week after TBI (Figure 1(a)). ALDOC and GS were persistently elevated up to five days post injury, while GFAP and S100 β decreased on the second post-injury day. Injury day BLBP and PEA15 levels were high, but varied on subsequent days (Figure 1(a)). APOB levels fluctuated together with those of BLBP and PEA15 (Figure 1(a)). This patient had an ischemic episode on the third post-injury day that coincided with a spike in these markers' levels. The CSF from a control subject had high levels of PTGDS, whereas PTGDS was not detected on injury day and its levels recovered over subsequent days in the CSF of a TBI patient (Figure 1(a)).

Sub-saturated CSF immunoblotting densitometry showed mean increases in TBI subjects of three (GFAP, S100 β, GS and BLBP) to four (ALDOC) orders of magnitude, while PEA15 and APOB were not detected in control subjects (Figure 1(d) to (j)). Median GFAP CSF levels increased most on injury and initial post-injury day followed by significant decreases on and after the second post-injury day (Figure 1(d)). S100 β signals varied more, but showed a similar decrease over time (Figure 1(e)). In contrast, most patients' ALDOC levels remained elevated over the five days examined post injury (Figure 1(f)). The two patients without measurable ALDOC also had lowest or no signals for all other measured injury markers and low overall protein concentrations. GS and BLBP varied more between TBI patients, yet also without significant mean decreases on later post-injury days (Figure 1(g) to (h)). PEA15 had the most heterogeneous signals across TBI patients, with mean elevation over controls on indicated days after TBI (Figure 1(i)). Similar to GFAP, mean APOB levels were highly elevated on the first two injury days in the TBI cohort, followed by variable decrease and significantly lower means four and five days post injury (Figure 1(j)). Mean PTGDS levels were invariably high among controls and decreased significantly after TBI on early post-injury days (Figure 1(k)). Preliminary analysis of this cohort shows that mean PTGDS levels recovered in TBI survivors, while levels declined further in nonsurvivors (Supplementary Figure S4(a)).

We also identified and measured trauma-generated small GFAP breakdown products (BDPs), of 18, 20 and 25kD in size that are new to the TBI field. CSF levels of small GFAP BDPs varied over time and between patients (Figure 1(a) and (b)). In this small cohort, preliminary comparisons between survivors and nonsurvivors show a 10-fold greater survival difference for small GFAP BDPs than for total GFAP signals, suggesting that small GFAP BDPs improved survival prediction (Supplementary Figure S4(b)). Half of the TBI CSF samples also displayed a trauma-generated 38 kD ALDOC fragment that appeared predominantly on later post-injury days (Figure 1(c)). Overall, AID biomarkers displayed extended longitudinal CSF presence compared to previously known astroglial biomarkers, and variation in their longitudinal profiles documents that different kinetics exist among astroglial biomarkers.

AID biomarker concentrations are measured using protein and peptide-based approaches

Quantitative mass spectrometry via MRM-MS was used to systematically quantify several biomarkers in TBI patients (Figure 2). MRM-MS uses ratios between peptides from CSF-derived endogenous proteins and internal standard isotope-labeled peptides to determine biomarker concentrations. From MRM-MS measurements, GFAP and ALDOC had greater levels in TBI CSF than in control CSF (Figure 2(a); similar data for PEA15, BLBP and GS are not shown). In addition, longitudinal CSF profiles showed matching trends between immunoblot and MRM-MS measurements for a severe TBI survivor, as documented for GFAP and ALDOC (Figure 2(b); BLBP and GS also had matching longitudinal trends between the two methods, not shown). Immunoblot densities correlated well with MRM-MS measurements, as shown for GFAP (Figure 2(c)). MRM-MS allowed comparison of astroglial biomarker concentrations independent of using antibodies, yielding differences between biomarkers over four orders of magnitude. Injury day CSF levels were highest for ALDOC with GFAP next in order, while BLBP and GS levels were significantly lower (Figure 2(d)). By the third post-injury day, ALDOC concentrations were significantly (10-fold) above those of GFAP (Figure 2(e)). Known amounts of marker-specific peptides for MRM-MS and recombinant protein isoforms for immunoblots were used to estimate concentrations (see Supplementary Methods). Comparison of concentration estimates between the two methods showed similar detection limits and interquartile concentration ranges for ALDOC, BLBP and GFAP, further validating the trends obtained by both approaches (Figure 2(f)). The wide dynamic range of TBI biomarker concentrations reflects large clinical TBI heterogeneity.

Pairwise correlations and factor analysis reveal two divergent biomarker groups, each with similar TBI CSF kinetics

A comparison of biomarker levels for covariant and divergent profiles produced strongest correlation between small GFAP-BDPs, APOB and S100 β that may reflect an association between blood presence in

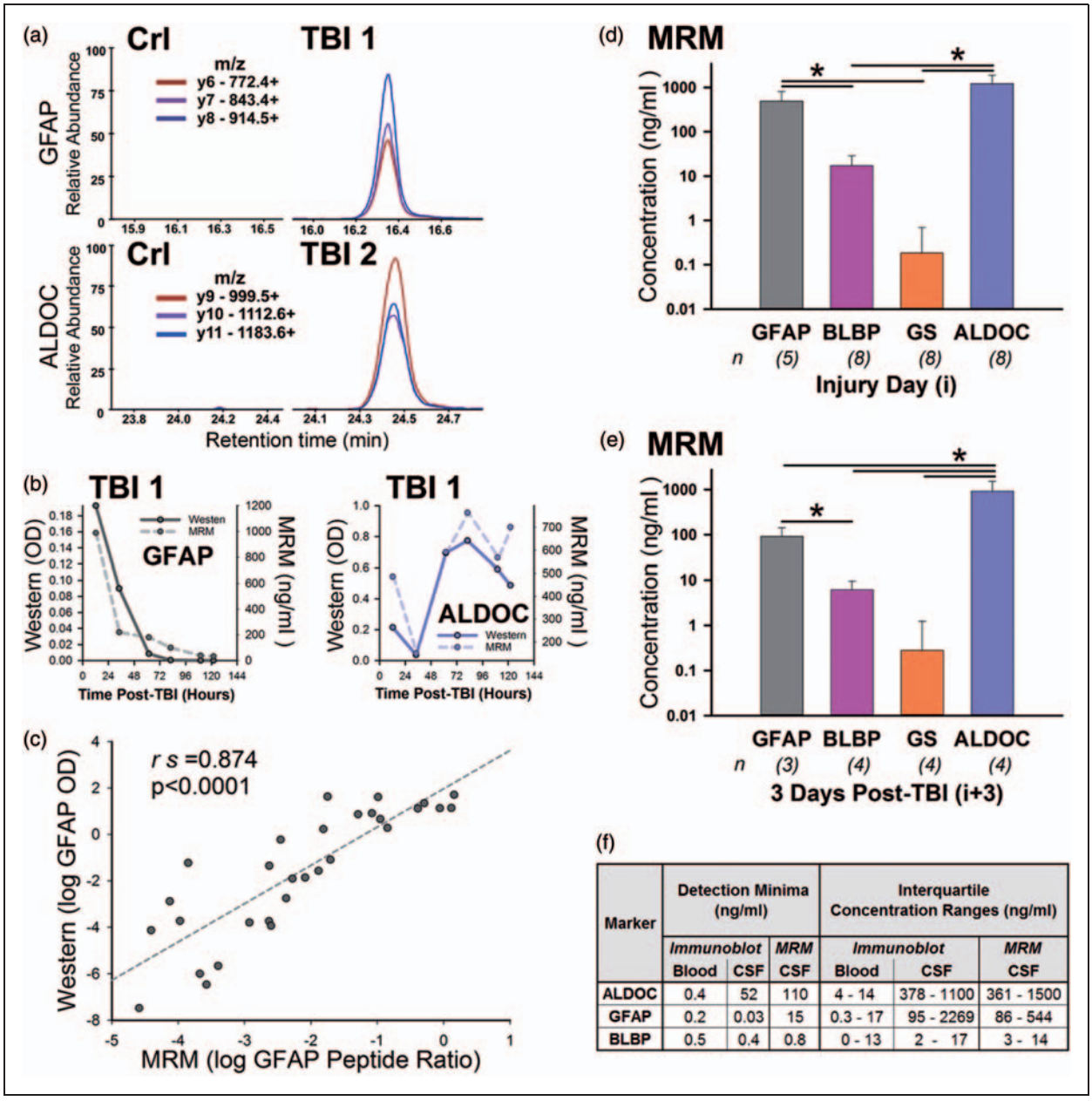

(f)

Marker	Detection Minima (ng/ml)			Interquartile Concentration Ranges (ng/ml)		
	Immunoblot		*MRM*	*Immunoblot*		*MRM*
	Blood	CSF	CSF	Blood	CSF	CSF
ALDOC	0.4	52	110	4 - 14	378 - 1100	361 - 1500
GFAP	0.2	0.03	15	0.3 - 17	95 - 2269	86 - 544
BLBP	0.5	0.4	0.8	0 - 13	2 - 17	3 - 14

Figure 2. MRM mass spectrometry and concentration comparison of AID biomarkers. (a) MRM-MS traces biomarker-specific peptides for GFAP and ALDOC in severe TBI CSF (TBI 1, 2) and from a control (Crl). Three product ion traces (y6-11) with given mass over charge (m/z) values and retention times (min, x-axis) are shown. They are from precursor ions with m/z 549.816 (GFAP) and m/z 526.970 (ALDOC). (b) Immunological and mass spectrometry measurements show comparable TBI CSF temporal profiles for GFAP and ALDOC in longitudinal CSF samples of a severe TBI patient (TBI 1). Biomarker levels were measured using immunoblot densitometry (continued lines show ODs, left y-axes) and multiple reaction monitoring-mass spectrometry, MRM-MS (dashed lines, ng/ml, right y-axes). (c) Biplot shows TBI patients' CSF log MRM-MS data for the GFAP peptide using endogenous divided by standard ion transition ratios (x-axis) and GFAP log immunoblot ODs (y-axis) with regression line and Spearman correlation ($r_s = 0.874$, $p < 0.0001$) to demonstrate strong agreement between the two methods. (d) Mean MRM-MS concentrations for GFAP, BLBP, GS and ALDOC in TBI CSF on injury day (n = patient numbers). ALDOC had 2.5-fold higher concentrations than GFAP on injury day (not significant). GFAP and ALDOC concentrations were over two orders larger than those of BLBP ($p < 0.001$) and over three orders higher than those of GS ($p < 0.002$). (e) Mean MRM-MS biomarker CSF concentrations on the third post-injury day after TBI. Mean ALDOC concentration was 10-fold higher than that of GFAP ($p = 0.008$). BLBP levels were lower than those of ALDOC and GFAP ($p < 0.001$) and ALDOC levels were three orders larger than those of GS ($p = 0.02$). (f) ALDOC, GFAP and BLBP interquartile concentration ranges were estimated from immunoblot densities using known amounts of pure proteins and calculated from MRM-MS signals using known amounts of isotope-labeled biomarker-specific peptides as standards. Reported detection thresholds are from 30 μl analyzed in immunoblots and 2 μl in MRM-MS.

CSF and astroglial demise (Spearman rank correlation coefficients, see Supplementary Table 7). BLBP and PEA15 correlated robustly with each other as did ALDOC and GS, indicating similar kinetics between these marker pairs. ALDOC correlated poorly with GFAP and S100 β, reflecting different temporal profiles. Astroglial biomarker levels correlated negatively with PTGDS, representing injured versus healthy conditions. Proteolytic fragments for ALDOC and GFAP did not covary, implying different proteolytic degradation kinetics (Supplementary Table 7).

Beyond pairwise comparison, iterative EFA simplified profiles of 10 markers, clustering them by underlying relationships as previously done with TBI patient comorbidities.[46] This unsupervised analysis grouped nine neurotrauma markers into two factors, with CSF standard PTGDS resulting in a third factor. Altogether, the three factors accounted for 84% of the cohort's data variance. Factor A comprised GFAP, its lower BDPs, S100 β and APOB, while Factor B contained ALDOC, its 38kD fragment, BLBP, GS, and PEA15 (Figure 3(a)). Each biomarker

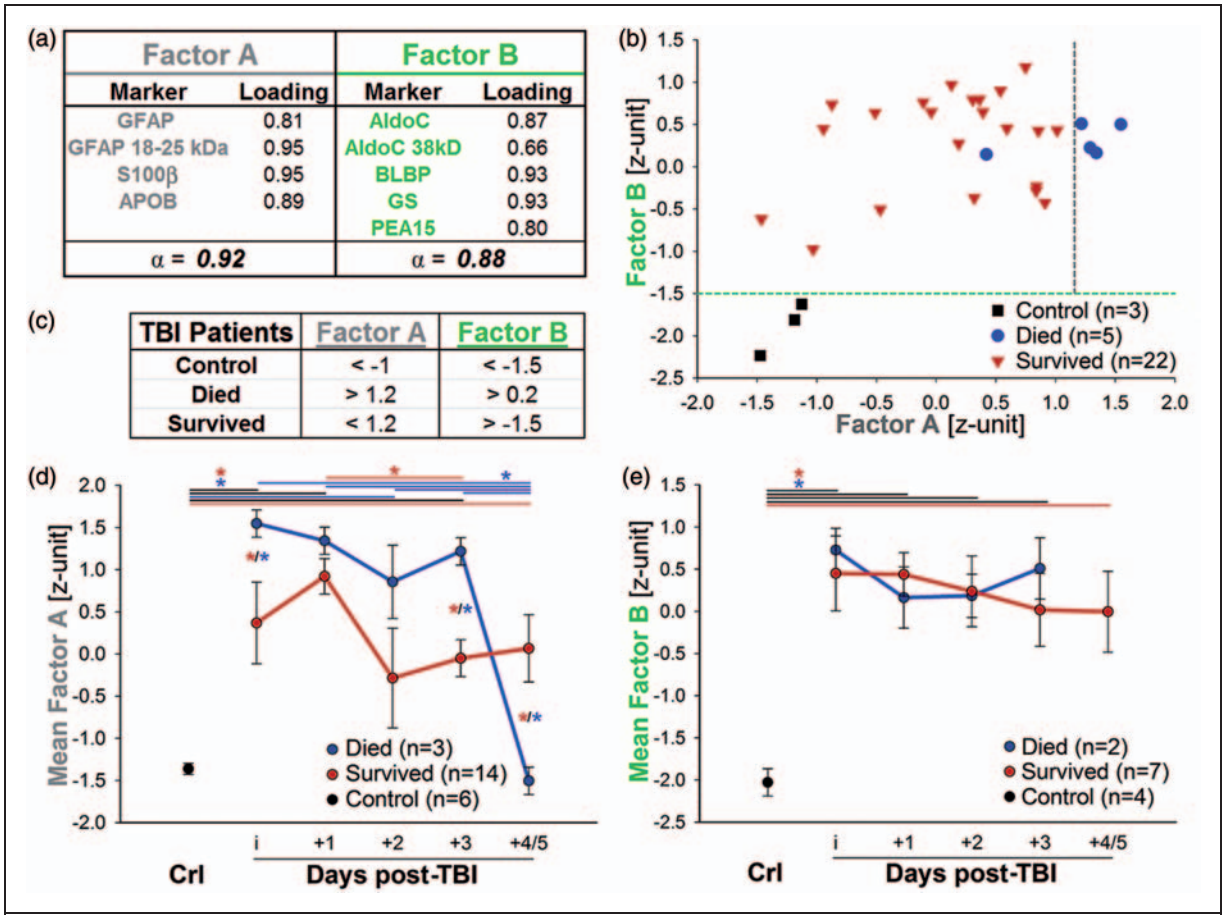

Figure 3. Exploratory factor analysis simplifies and classifies the biomarker panel based on different CSF kinetics. (a) Unsupervised exploratory factor analysis (EFA) grouped biomarkers S100 β, GFAP, small GFAP-BDPs and APOB into Factor A (gray) and ALDOC, ALDOC-BDP, BLBP, GS and PEA15 into Factor B (green). Each biomarker's loading and both factors' correlation coefficient (Cronbach's α) document strong inter-relatedness of biomarkers within each factor. (b) The biplot combines signals from nine biomarkers, giving CSF levels in z-units from 12 subjects with Factor A on x-axis and Factor B on y-axis. The Factors partitioned control from TBI using a Factor B threshold (green dashed line) and survivors from nonsurvivors of TBI using a Factor A threshold (gray dashed line). n = number of observations with available readings for all nine biomarkers. (c) Table reports the classification tree boundaries (factor thresholds, z-units) for partitioning between control subjects, died and survived TBI patients. (d) Longitudinal profiles of Factor A standardized means are plotted for survivors (red) and nonsurvivors (blue) of TBI over five post-injury days, documenting a significant decrease from injury day onwards, indicated with lines for respective groups (black = all TBI, $p < 0.005$). Factor A differed between TBI survivors and nonsurvivors significantly on post-injury days marked with double-asterisks (*/*, $p < 0.03$, effect size = 1). (e) Factor B means were elevated in TBI versus controls ($p < 0.001$), remained elevated over five post-injury days but did not differ with respect to survival; n = number of subjects.

had high loading to its respective factor, documenting strong correlation between biomarkers grouped together by EFA. The factor coefficient alpha was high as well, further describing close underlying relationships of the biomarkers within each factor (α, Figure 3(a)). As shown in the following sections, some of these relationships were investigated. The two-dimensional factor biplot condensed trends across all nine biomarkers to concisely document the heterogeneity among TBI patients (Figure 3(b)). Classification tree analysis using factor boundaries separated controls, TBI survivors and nonsurvivors. CSF levels for Factor A decreased significantly over post-injury days, while Factor B profiles did not, suggesting faster CSF clearance of Factor A biomarkers and more stable Factor B biomarkers (Figure 3(d) and (e)). Factor A had significant difference on injury day between survivors and nonsurvivors that could improve early outcome prediction; this difference is further documented by partitioning lines in the scatterplot based on thresholds obtained by classification tree analysis (Figure 3(b) to (d)). Thus, EFA succinctly summarized nine biomarker profiles and revealed key kinetic differences between two biomarker groups. Biomarker release and clearance were subsequently investigated in blood profiles after TBI as well as in a trauma model.

Early AID biomarker blood elevation after severe and mild TBI are unique

Blood samples from 22 severe TBI patients of the aforementioned cohort were analyzed alongside 12 control subjects and 15 mild TBI patients (Figure 4). BLBP and PEA15 were detected in the earliest severe TBI serum sample (3 h post injury) prior to their detection in the same patient's CSF (Figure 4(a)). In contrast, small GFAP-BDPs were elevated in CSF before their appearance in circulation, coinciding with clearance of GFAP from CSF (Figure 4(a)). The 25 kD GFAP fragment was consistently absent from blood on injury day and appeared robustly one day post injury in the entire TBI patient cohort (Figure 4(c) and (d)). ALDOC signals were present at 3 and 34 h in same patients' CSF and blood (Figure 4(a)), confirming recent findings of serum ALDOC using proteomic profiling after rat controlled cortical impact.[47] Cohort ALDOC blood levels were consistently elevated for all five post-injury days, rising significantly between injury day and two days post injury (Figure 4(c) and (e)). Mean injury day levels for BLBP and PEA15 were significantly elevated over control levels but were less frequently elevated on later post-injury days (Figure 4(c), (f) and (g)). ALDOC, GFAP 25 kD fragment and BLBP interquartile concentration ranges were estimated in the tens of nanograms (Figure 2(f)). Together, the data suggest differences in release and circulation kinetics among these four astroglial biomarkers.

Greater presence of AID biomarkers on injury day in 15 mild TBI patients than in controls is documented. Robust elevation of the biomarkers in serum from mild TBI subjects was detected at the earliest available time (1 h after mild TBI) for ALDOC, BLBP and PEA15 (Figure 4(h)). ALDOC was present in 80%, BLBP in 47% and PEA15 in 60% of this mild TBI cohort regardless of CT-scan status. Noticeably, levels of the 25kD-GFAP-BDP were zero or very low and were detected only in 13% of the samples, consistent with recent findings.[48] Interestingly, several injury day mild TBI sera positive for ALDOC, BLBP and PEA15 had signals of comparable strength to those typically observed in injury day severe TBI blood (Figure 4(c) and (h)). Taken together, ALDOC, PEA15 and BLBP had profiles distinctly different from those of GFAP BDPs in severe TBI patients. These observations led us to investigate early cellular post-injury biomarker release in an in vitro human trauma model.

Traumatized human astrocytes show membrane wounding, reactivity and cell death at different times post injury

Differentiated, serum-free human astrocytes grown on deformable membranes received pressure-pulses that produced diffuse shear-stretch injuries reminiscent of an abrupt traumatic force.[35,49] Subpopulations of traumatized human astrocytes (1) displayed membrane wounding, (2) died or (3) became reactive, as indicated by star-shaped morphology and GFAP upregulation[35,36] (Figure 5). Wounded cells displayed beaded, fragmented or amputated processes with elevated GFAP signals already at 30-min post stretch, prior to reported GFAP gene expression changes[36,50] (Figure 5(c)). Intact, wounded and demised astrocytes were counted by distinguishing characteristic nuclear shapes, and live dye-uptake was used to assess membrane integrity (see Methods). The population of membrane-wounded cells increased significantly by 30 min after injury, with similar means after mild and severe stretches (Figure 5(e)). Their numbers decreased substantially by two days (2d) after stretching (Figure 5(e)). In contrast, cell death rates were low at 30-min post injury and rose to substantial levels by 2d post injury, at which point they differed significantly between mild and severe pulses (Figure 5(f)). Thus, cell death in this human trauma model reflected two distinct outcome-defined severities. Furthermore, temporal distinction between cell wounding and cell death allowed correlation of biomarker release with cellular injury states after trauma.

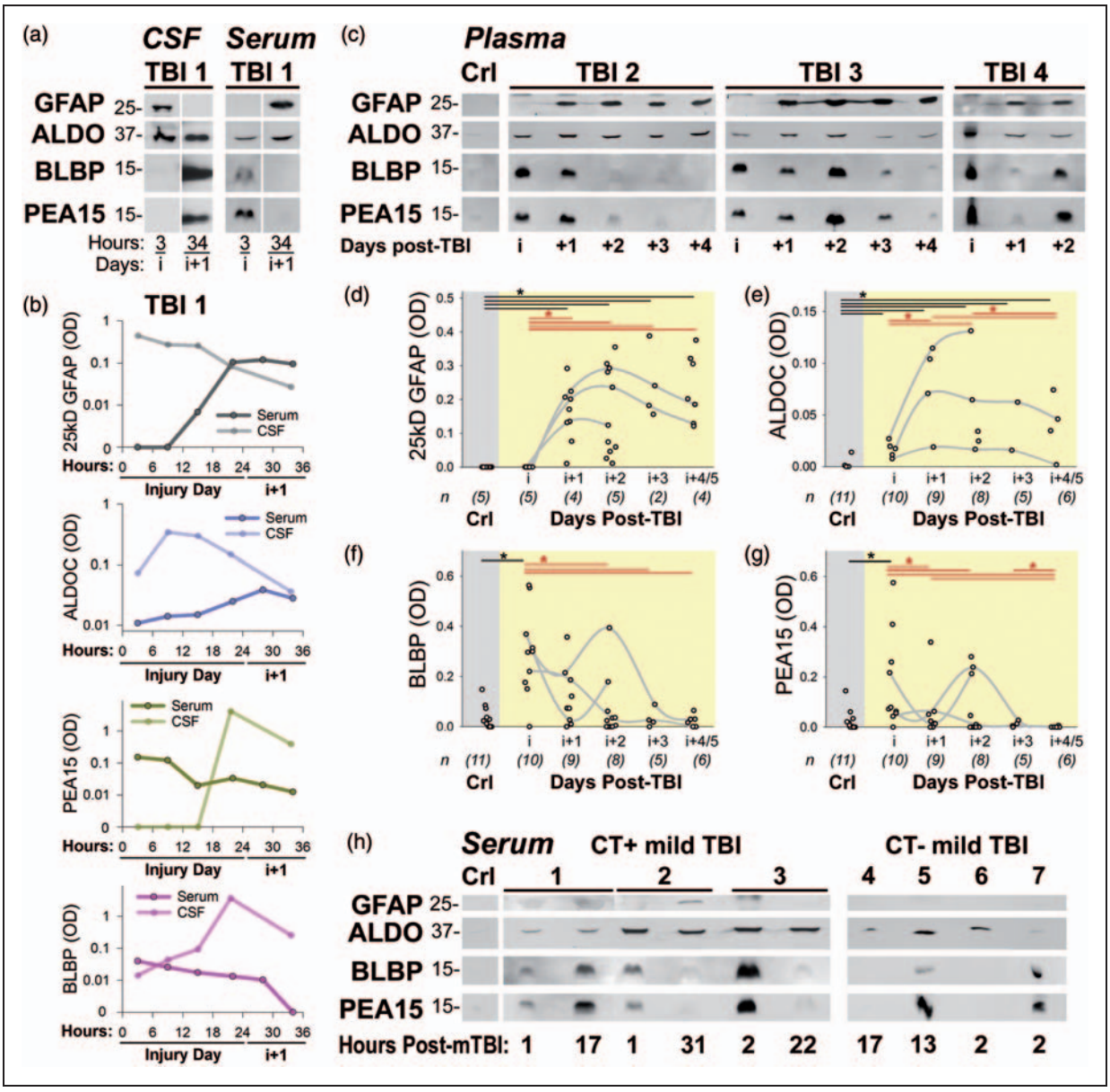

Figure 4. AID biomarkers appear hyper-acute and robust in blood of severe and mild TBI patients. (a) Immunoblots show that small GFAP-BDPs, ALDOC, BLBP and PEA15 appear in CSF and serum at different times when compared in one severe TBI patient (TBI 1) at 3 and 34 h post injury (i and i + 1). (b) Temporal profiles of same markers are plotted for concurrent CSF (light lines) and serum (dark lines) samples of the same patient. Biomarker increase in serum correlates with decrease in CSF. ALDOC, PEA15 and BLBP were present in serum earlier than GFAP. (c) Immunoblot of 30 µl depleted plasma samples show signals for 25kD-GFAP-BDP, aldolase A + C (ALDO, mab E9), PEA15 and BLBP in three severe TBI patients on injury day and two to four post-injury days (TBI 2, 3, 4). Corresponding signals are absent in control. (d–g) Scatterplots show biomarker levels in plasma with temporal profiles for (d) 25 kD-GFAP-BDP, (e) ALDOC (isoform-specific mab 5C9), (f) BLBP and (g) PEA15. Consecutive samples from the same patient are connected by a gray line. (d) 25 kD-GFAP-BDP was absent on injury day in all TBI patients, but was elevated on post-injury days 1–5 ($p < 0.0001$). (e) ALDOC levels were elevated on TBI injury day by 88-fold over control (black lines, asterisk, $*p < 0.027$). On the following two post-injury days, ALDOC levels rose > 300-fold over controls (black lines, asterisk ($*p < 0.009$) with levels on i + 1 and i + 2 significantly above those of injury day (red lines, asterisk: $*p < 0.027$). On i + 3 and i + 4, ALDOC mean levels decreased (red lines, asterisk, $*p < 0.05$). (f) Mean BLBP levels were elevated on injury day by 122-fold (black line, asterisk, $*p = 0.007$), remained elevated on i + 1 and decreased subsequently (red line, asterisk, $*p < 0.02$). (g) PEA15 levels increased on TBI injury day by 40-fold (black line, asterisk, $*p = 0.02$) and decreased thereafter (red line, asterisk, $*p < 0.04$). (h) Immunoblots show 30 µl depleted serum samples from mild TBI patients at early post-injury hours. The same film exposures are shown for mild and severe TBI samples. In mTBI, ALDO (mab E9), BLBP and PEA15 signals co-varied, while 25 kD-GFAP-BDP signal was weak or absent. mTBI patients one to three had reported CT scan findings (CT-positive, +) while mTBI four to seven had no brain injury-associated CT findings (CT-negative, −). See Supplementary Table 1(c) for mTBI patient details.

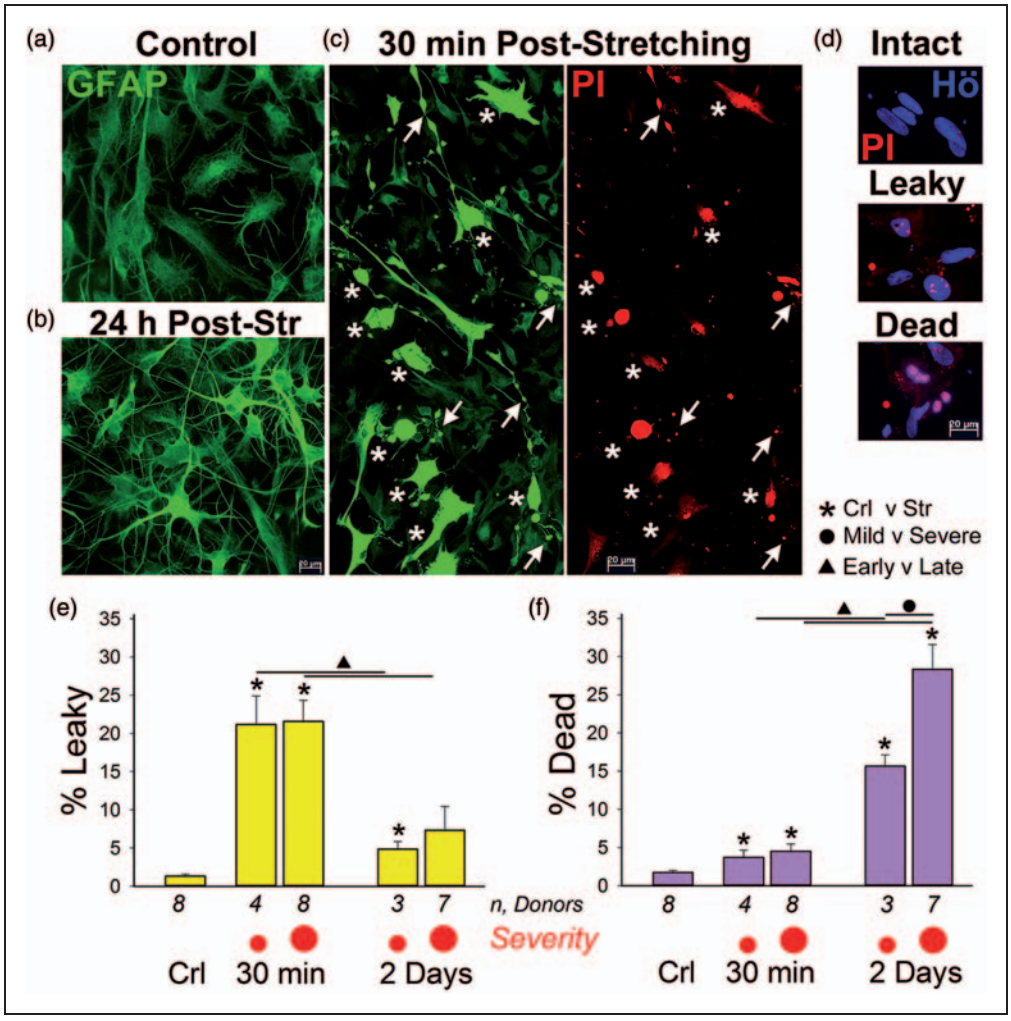

Figure 5. Mechanical trauma causes acute membrane wounding, reactivity and delayed cell death in human astrocytes. (a) GFAP (green) is weakly expressed in uninjured, differentiated neocortical human astrocytes. (b) Reactive astrocytes 1d post injury were star-shaped with enlarged processes and upregulated GFAP. (c) Acutely wounded, mechanoporated astrocytes 30 min after stretching had bright GFAP signals and beaded, disintegrated (arrows) or amputated (*) processes in cells that had taken up PI (red). (d) Nuclear morphologies distinguish intact cells with large, oval-shaped Höchst-stained nuclei (pale blue). Leaky, membrane-wounded astrocytes had same shape and Höchst-stained nuclei but with PI-positive nucleoli (pink). Dead astrocytes had small nuclei with condensed chromatin (pyknotic), which were bright Höchst- and PI- stained (pink). (e) Counted leaky cell medians were elevated at 30 min ($p < 0.0001$) and 2d post injury ($p < 0.01$) after mild (2.6–4.0 PSI, ●, small red dot) and severe (4.4–5.3 PSI, large red dot, ●, $p < 0.001$) stretching. Leaky-cell fractions decreased between 30 min and 2d post injury (Δ, $p < 0.01$). (f) Median cell death numbers were slightly elevated at 30 min (*$p < 0.05$, mild; *$p < 0.01$ severe). Cell death substantially increased by 2d after stretching from 30 min (Δ, $p < 0.0001$, 2d difference to unstretched were *$p < 0.01$, mild; *$p < 0.001$, severe). A severity difference in cell death means was found at 2d post injury between mild and severely stretched cultures (indicated by a black dot • $p < 0.001$).

Biomarkers and their release kinetics correlate with astrocyte wounding and cell death

Immunoblotting of conditioned media (fluid) from control and stretched astrocyte cultures shows intact GFAP only immediately after severe stretching. Small proteolytically-generated GFAP BDPs (18, 20 and 25 kD) appeared one to two days after injury (Figure 6(a)). In contrast, ALDOC, BLBP and PEA15 were already robustly released 30-min post injury (Figure 6(a)). Sub-saturated immunoblot densitometry from control and four post-injury time points documents exponential biomarker elevation with mean levels rising over three orders of magnitude (Figure 6(b) to (e)). GFAP levels increased five-sevenfold over time post injury ($p < 0.013$) and showed a fivefold severity difference at 5 h post stretch ($p = 0.042$, Figure 6(b)). In contrast, ALDOC, BLBP and PEA15 levels rose already 30 min after mild stretching (60-460-fold, $p < 0.0001$) but were not significantly different (two-threefold) from severe stretching.

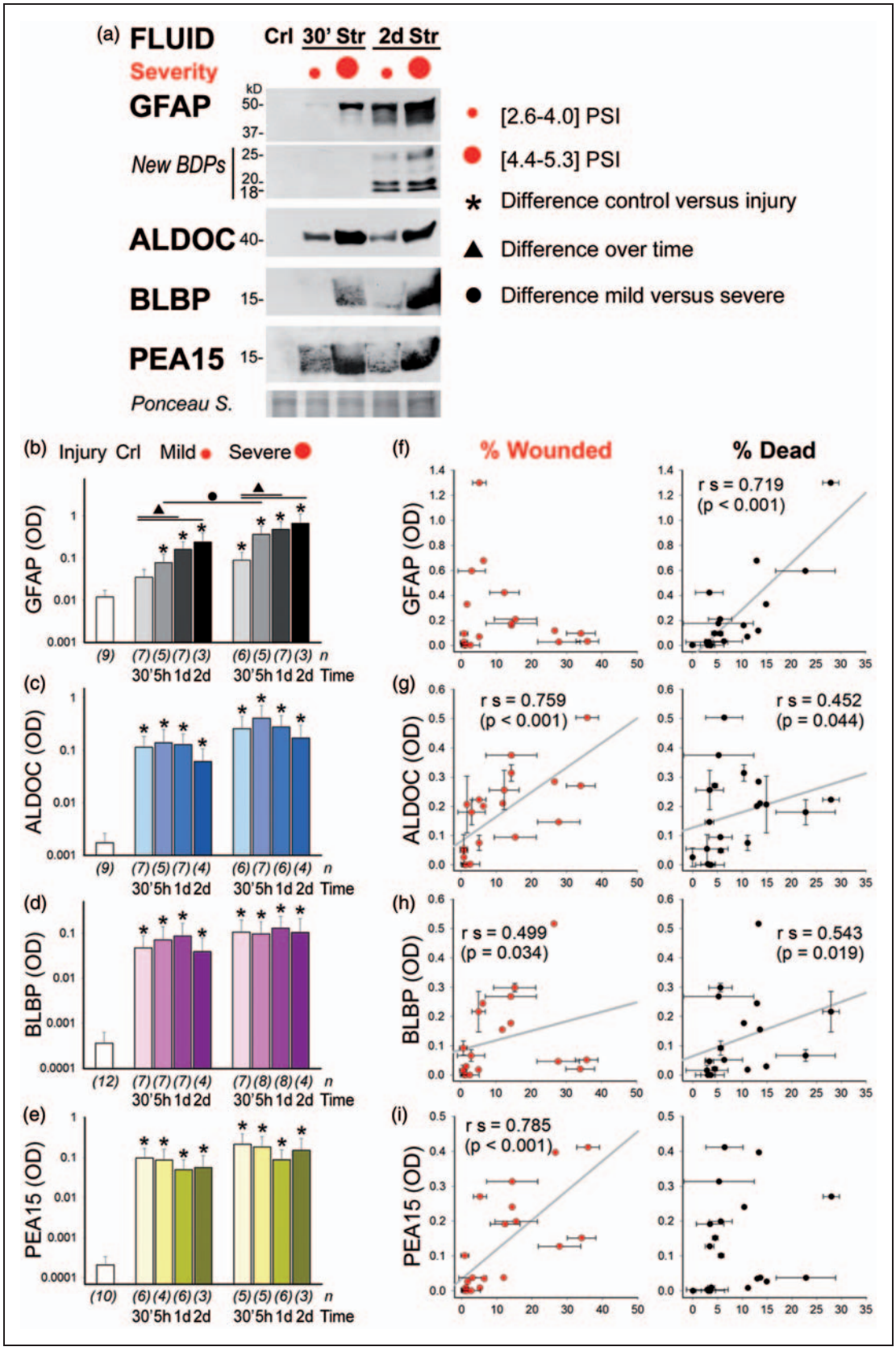

Figure 6. Human astroglial biomarker release is defined by membrane wounding and cell death after mechanical trauma. (a) Immunoblots from concentrated conditioned medium (fluid) of unstretched (control, Crl), mild stretched (2.6–4 psi, small red dot, •)

Further, their levels remained similarly elevated at all time points post injury after mild and severe stretching (Figure 6(c) to (e)). This suggests that release of cytosolic biomarkers ALDOC, BLBP and PEA15 was related to both early cell wounding and later cell death, while the release of cytoskeletal GFAP, particularly its small BDPs, corresponded selectively with delayed cell death. To further investigate this finding, each biomarker's levels in fluid were plotted against cell wounding and cell death rates, and their Spearman correlations were determined (Figure 6(f) to (i)). ALDOC and PEA15 associated strongly and BLBP moderately with cell wounding. ALDOC and BLBP also correlated moderately with cell death. GFAP had the strongest correlation with cell death and did not correlate with cell wounding. This is the first report of fast ALDOC, BLBP and PEA15 release due to cell membrane wounding after mild and severe human astrocyte trauma, and it is the first to selectively relate GFAP, particularly its small fragments, with astroglial death.

Trauma causes astroglial protein depletion and disassembly in wounded and dying cell populations

To begin addressing the striking difference in biomarker release kinetics and to further understand the relationship between fluid levels and cell injury states, we combined membrane leak (or wounding, tracked by dye-uptake) and biomarker immunofluorescence at 30-min post injury. Viable GFAP-expressing control astrocytes had typical fibers of cytoskeletal filaments. These fibers disappeared acutely after stretching and GFAP signal appeared homogeneous (Figure 7(a)). This pattern change was scored, documenting a significant increase in cells with GFAP fiber loss observed predominantly in leaky astrocytes (Figure 7(i) and (e)). Control GFAP-expressing astrocytes had brighter BLBP signals than those 30-min post stretch (Figure 7(b) and (k)). Stretched astrocytes with dimmed BLBP signals still retained noticeable GFAP signals with disassembled appearance (Supplementary Figure S5). The number of bright BLBP-stained cells decreased significantly 30 min after stretching (Figure 7(f), (j) and (k)). ALDOC and PEA15 were ubiquitously expressed in control astrocytes, and their signals decreased in a fraction of leaky cells 30 min after stretching (Figure 7(c), (d) and (k)). Some leaky cells showed blebbing, a sign of plasma membrane irregularity (Figures 7(c)). Thirty minutes after stretching, ALDOC and PEA15 depletion occurred in 29–39% of leaky cells and in 11–14% of intact cells, which could have resealed by 30 min after initial leakiness post stretch (Figure 7(g) and (h)). Single cell biomarker immunofluorescence intensity measurements documented acute and significant cellular marker loss 30 min after stretching for BLBP (by 29%), ALDOC (by 34%) and PEA15 (by 43%, Figure 7(k), $p < 0.001$).

These cellular studies document for the first time a subpopulation of wounded human astrocytes that contributes to early biomarker increase measured in fluids. This evidence further supports the new concept that hyper-acute release of cytosolic markers ALDOC, BLBP and PEA15 originated from wounded human astrocytes post trauma without substantial cell death. In contrast, GFAP was temporarily retained but underwent cytoskeletal filament loss before its delayed release and proteolytic cleavage with cell death. These trauma-inflicted release kinetics highlight different post-injury stages, classifying astroglial biomarkers into two groups based on different cellular injury processes.

Culture trauma model findings echo clinical biomarker profiles

The in vitro trauma model revealed significant differences in GFAP release and its cleavage that correspond well with the different cell death rates documented for the two pressure ranges and reflect different severities in the culture model. GFAP levels in TBI patients predicted outcome, as shown here and in many studies

Figure 6. Continued
and severe stretched (4.4–5.3 psi, large red dot, ●) astrocyte cultures are shown at 30 min (30′) and 2d post injury. Blots show fluid signals for GFAP, ALDOC, BLBP and PEA15. Small GFAP-BDPs (25–18 kD) were absent at 30 min and present by 2d post injury, whereas ALDOC, BLBP and PEA15 were present 30 min post injury and at 2d. Ponceau S shows total protein amount for 30 µl fluid per lane. (b–e) Geometric means of optical densities (OD) for (b) GFAP, (c) ALDOC, (d) BLBP and (e) PEA15 are plotted for unstretched, 30 min, 5 h, 1d and 2d mild and severe stretched cultures. All stretched fluid samples show significant biomarker elevation compared to those of unstretched fluids (*GFAP 5 h mild stretch: $p = 0.005$, all others $p < 0.001$; n = number of donors).
The exception was that GFAP elevation in fluids was only threefold ($p > 0.05$) 30 min after mild stretching. In contrast, 30-min mild stretched cultures had significantly elevated levels of ALDOC (66-fold), BLBP (130-fold), and PEA15 (460-fold, all *$p < 0.001$). GFAP release levels increased over indicated times (see lines and ▲, $p < 0.02$). GFAP levels showed severity difference at 5 h after stretching (•, $p = 0.042$). Severity differences for ALDOC, BLBP and PEA15 were two-threefold and not significant. (f–i) Biplots correlate biomarker levels on y-axes with percent wounded astrocytes (red, leaky) and percent dead cells (black) on x-axes. Spearman correlations (r_s) are given with p-values and lines of best fit. Error bars are standard deviations of replicate analyses. (f) GFAP correlated only with cell death rates. (g) ALDOC and (h) BLBP correlated with cell wounding and cell death. (i) PEA15 correlated only with cell wounding.

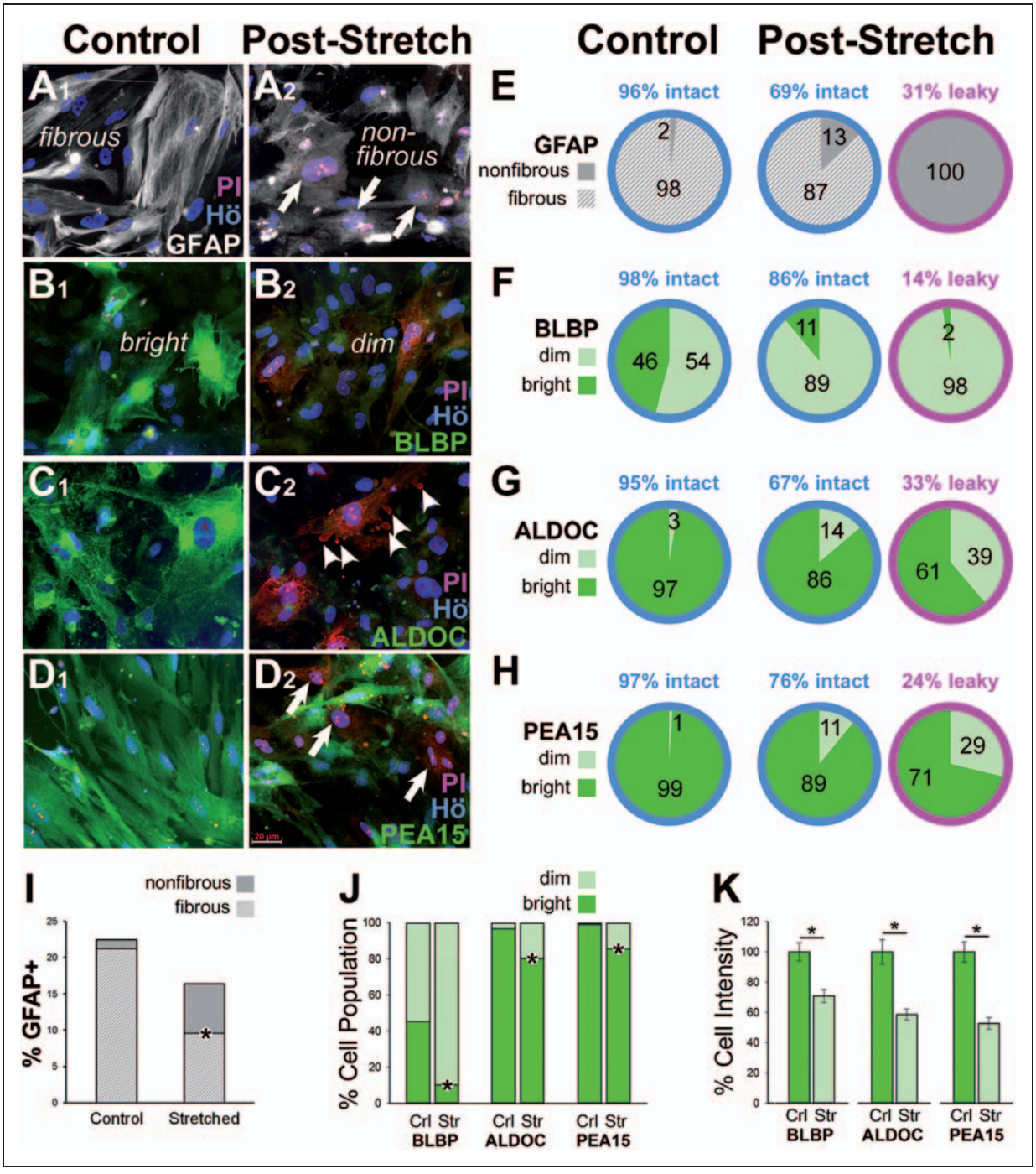

Figure 7. Acute cell wounding is associated with depletion of astroglial markers and GFAP filament disruption. PI-dye uptake for membrane leak was combined with biomarker immunofluorescence in control and stretched human astrocytes 30 min after injury. (A1) Intact PI-negative control astrocytes displayed filament-assembled fibrous GFAP (white). (A2) Leaky PI-positive astrocytes (pink in nuclei, arrows) had homogeneous non-fibrous GFAP. (B1) Control astrocytes show bright BLBP staining (green). (B2) Stretched leaky astrocytes had dim BLBP staining. Control cultures show ubiquitous (C1) ALDOC and (D1) PEA15 expression. (C2) Stretched cultures at 30 min post injury had leaky astrocytes (PI-positive, red, arrows) showing plasmalemmal blebbing (arrowheads) and dim ALDOC signals. (D2) PEA15 positive and negative cells were seen 30 min post stretch. Leaky PI-positive cells lacked PEA15 signals (arrows). (e–h) Pie charts show cell fate and marker scoring results corresponding to events in micrographs for four to seven cultures per condition and biomarker. (e) Proportions of fibrous (striped) and non-fibrous (gray) GFAP in populations of intact (blue ring) and leaky (pink ring) astrocytes. Stretching increased non-fibrous GFAP in intact/resealed ($p = 0.006$) and leaky populations ($p < 0.001$, $n = 5$). (f) The population of bright BLBP-stained, GFAP-positive astrocytes decreased 30 min after stretching and was nearly absent

(continued)

across the TBI spectrum.[51,52] On the other hand, acute release of ALDOC, BLBP and PEA15 was high, showing levels in the same ranges after mild and severe stretching. This could be explained by the similar mean percentages of acutely wounded cells between stretch severities. Notably, ALDOC, BLBP and PEA15 also displayed robust serum levels in mild TBI patients that were in the same ranges as those found in severe TBI patients' blood. Ultimately, the trauma model connected biomarker release to cell injury stages, resulting in marker groups that agreed with EFA factors derived from clinical CSF biomarker profiles. Together, our results yield neurotrauma biomarker groups defined by cell injury processes, i.e. membrane integrity compromise, and biofluid kinetics, including release, degradation and passage into circulation.

Discussion

A new panel of AID biomarkers was identified from our TBI CSF proteome using in vitro trauma-released and astrocyte-enriched proteins. Clinical studies established AID biomarker elevation with different post-injury kinetics in TBI patient biofluids. AID biomarkers were further distinguished by their release from either wounded or dying human traumatized astrocytes in a trauma model. This concordance led us to introduce a new concept for biomarker classification based on astroglial compromise and demise.

Need for unbiased and timely assessment of TBI patients

Presently, the initial assessment of TBI patients relies on GCS scores and CT scans, both of which correlate poorly with outcome and functional compromise after TBI.[7] Mild TBI victims are assessed using behavioral testing and cognitive questionnaires.[53] These tests rely on subjective self-reporting and require baseline assessment. An unbiased brain injury signature that can assess TBI patients and identify complicated injuries among mild TBI patients is required.[54] On-site and urgent care diagnosis of TBI patients, particularly of athletes and military personnel, would provide valuable objective advice on transportation and treatment choices. Connecting acute cellular injury processes with biomarker release and concomitant presence in the circulation are prerequisites for future real-time blood-based TBI patient assessment. Few animal studies address primary cellular injury events or early biomarker release.[55–58] After mild TBI, GFAP's passage into the circulation is delayed, limiting its benefit as an urgent care tool.[52] UCHL1 declines on injury day, restricting its later post-injury use.[52,59] These and other limitations account for the lack of a clinical diagnostic TBI test.[60] Our study addresses those current limitations, as ALDOC, PEA15 and BLBP are released nearly instantly upon impact, are elevated over an extended window after TBI and are present robustly after mild TBI.

Overcoming biomarker bottlenecks using a multiplex standardized TBI assay

Proteomics can provide a comprehensive view of protein changes after neurotrauma, yet clinically useful neurotrauma biomarkers remain elusive.[23,61] A major hurdle has been the selection of clinically relevant biomarkers from extensive lists of identified proteins, which our controlled human trauma model and selection strategy have cleared.[23,62] Non-standardized assays are a problem in comparing neurotrauma biomarkers.[63] Efficient throughput that measures multiple candidates requires a standardized approach.[64] MRM-MS is favored as a multiplex, antibody-independent assay for simultaneous measurement of multiple biomarkers. To our knowledge, it has not yet been applied systematically in the neurotrauma field.[54,63]

Astrocyte trauma responses are heterogeneous

We previously documented heterogeneity among astrocytes based on variable expression of astroglial markers and different trauma responses.[30,35] Morphological signs

Figure 7. Continued
in leaky cells ($p = 0.007$, $n = 5$, see Supplementary Figure S4 for biomarker double-labeling). (g) Most intact control astrocytes were ALDOC-positive (green). Stretching increased the fraction of ALDOC-depleted cells compared to controls ($p < 0.03$), with greater numbers of ALDOC-depleted cells among leaky than among resealed/intact subpopulations ($p < 0.001$, $n = 6$). (h) Most intact control astrocytes were PEA15-positive. Percentage of PEA15-positive astrocytes diminished 30 min after stretching ($p < 0.01$), with larger depleted fractions among leaky than among intact/resealed stretched cells ($p < 0.0001$, $n = 6$). (i) Percent GFAP-expressing astrocytes with fibrous and non-fibrous patterns in control and in acutely post-stretch astrocytes are plotted. The shift from fibrous to non-fibrous GFAP was significant early post injury ($^*p < 0.01$), but the reduction of overall GFAP-expressing cells was not significant. (j) Percentages of cells with bright and dim biomarker signals differed between control and 30-min post-stretch cultures for BLBP ($^*p = 0.007$), ALDOC ($^*p = 0.001$) and PEA15 ($^*p = 0.003$). (k) Single-cell measurements of immunofluorescence intensities show the decrease in BLBP, ALDOC and PEA15 signals 30-min post injury versus signals in control cells ($^*p < 0.001$, n = 3–5 cultures).

of astrocyte wounding were found early and were scattered in stretch-injured cultures, possibly reflecting both selective astrocyte vulnerability and 'hot spots' of focal tensile forces. While distinct subpopulations of wounded human astrocytes underwent depletion of cytosolic markers and GFAP filament disassembly, adjacent cells appeared unchanged, illustrating diffuse injury distribution. Rapid cell membrane wounding was associated with GFAP filament disassembly and brighter GFAP immunofluorescence signals. This new observation in mechanically wounded astrocytes preceded reported GFAP gene expression changes in reactive astrocytes.[30,50] Similarly, rapid alteration in GFAP antigenicity is found after acid treatment due to elevated calcium and is associated with calpain activation.[65,66] Cytoskeletal filament disassembly could contribute to the vulnerability of mechanoporated astrocytes, particularly to secondary insults.

Mechanical trauma-induced reactivity includes specific shape changes and upregulation of astroglial markers. It occurs within hours and evolves over days post injury in human astrocytes.[35] Trauma-induced transcription factor STAT3 upregulates expression of GFAP, ALDOC, BLBP and PEA15 during reactive gliosis.[28,30,67] Their reactive upregulation may amplify secondary release associated with injury progression. Thus, it is important to distinguish different astrocyte cell fates after trauma-acute membrane wounding, astrogliosis and delayed astroglial demise, each of which exhibit distinct temporal profiles and are different aspects of neurotrauma.

AID biomarkers monitor acute trauma pathology of astroglial membrane wounding and fiber damage relevant to mild TBI diagnosis

Mechanoporation, or plasmalemmal permeability, is an early and enduring pathology in acutely traumatized CNS tissues and is also a hallmark of diffuse axonal injury, characterized by process beading and fragmentation.[10,11,68] Diffuse white matter damage is seen in mild TBI patients with post-concussive symptoms.[69] How long mechanoporated cells endure in a compromised state and whether they recover or undergo subsequent cell death are open questions.[70] Acutely traumatized astrocytes showed integrity compromise and process damage in this trauma model. In vivo astroglial fiber damage, clasmatodendrosis, is reported after mouse spinal cord injury as well as in the traumatically injured primate and human cortex and is associated with protein degradation.[13,30,71] Astrocytes outnumber neurons in human neocortical white matter, and human astrocytes carry oversized processes, manifesting their clinical relevance to white matter health.[27,72] Thus, astroglial wounding-released biomarkers ALDOC, BLBP and PEA15 provide the potential for diagnostic insight into the pathophysiology of diffuse glial fiber damage acutely after mild and severe TBI that goes beyond tissue demise. In vitro and in clinical biofluids, acute marker elevation supports a scenario in which traumatic impact, whiplash or blast produces an initial wave of mechanoporation. Future studies will determine the eventual fate of these cells and their relevance for TBI outcomes. The clear presence of ALDOC, BLBP and PEA15 in several mild TBI patients as opposed to GFAP's absence or scarcity makes wounding markers more likely to be diagnostically useful for assessing mild TBI patients.

Astroglial depletion of AID biomarkers may contribute to metabolic depression

Astrocytes maintain high rates of active oxidative glucose metabolism, express high levels of glycolytic and tricarboxyl acid cycle enzymes and carry many mitochondria.[26,31] GS and BLBP have vital roles in glutamate recycling and fatty acid uptake at the tripartite synapse.[73,74] ALDOC provides the substrate for lactate and ATP production and its product glyceraldehyde-3-phosphate controls cell fate and astrocyte-neuron crosstalk.[75] PEA15 regulates glucose metabolism, provides resistance to glucose deprivation and adapts cells to changing metabolic states.[76,77] Astrocytes can regulate neuronal metabolic supply by adjusting local blood flow on demand because they ensheath synapses as well as capillaries.[74,78] Thus, astroglial metabolism is essential for maintaining neuro-metabolic coupling and brain energy homeostasis.

As measured by positron emission tomography (PET) scans, many mild and severe TBI patients undergo metabolic depression with reduced cerebral oxidative metabolism and an imbalance of lactate, pyruvate, glutamate and glucose.[8,79,80] In a rat cerebral concussion model, metabolic depression after lateral fluid percussion is associated with altered astrocyte metabolism.[81–83] Selective depletion of metabolic enzymes and regulators may impair energy capacity of injured astrocytes and the neurons they supply. Our work provides the first evidence that ALDOC, BLBP and PEA15 release accounts for metabolic protein loss in subpopulations of traumatized human astrocytes. In vivo, ALDOC and PEA15 are also reduced in perilesional astrocytes acutely after mouse spinal cord injury.[30] The loss of these biomarkers from wounded astrocytes indicated by their elevation in fluid could contribute to metabolic depression in TBI patients.

GFAP release and degradation associate with astrocyte death after traumatic injury and predict survival after severe TBI

Severe TBI with lesions and contusions is associated with tissue demise, vascular damage, hemorrhage and

irreversible perilesional astrocyte swelling leading to cytotoxic edema.[84,85] Astrocyte demise is reported after cortical lateral fluid percussion in rats and one day after mouse spinal cord contusion.[86,87] Human post-mortem cerebral and hippocampal cell counts document severity-dependent progressive astroglial death at different mortality times after TBI.[88] Severity-dependent release of GFAP and S100 β after stretching of rat hippocampal slice cultures is documented, but hyper-acute changes were not investigated.[89] We show for the first time that cell death in human astrocytes had a considerable delay, was preceded by GFAP release, and coincided with the generation and release of small GFAP-BDPs. Thus, trauma-inflicted astroglial demise can be monitored using GFAP, and more selectively, its cell death-associated fragments, which better distinguished surviving from dying TBI patients. Severe TBI patients' CSF levels of proteolytic αII spectrin fragments also increase over time post injury and similarly differentiate nonsurvivors from survivors.[90] Together, the observations strengthen an association between cytoskeletal breakdown, cell death and mortality after TBI.

Astroglial neurotrauma biomarkers have kinetic diversity

Biomarker profiles fluctuate as a result of injury progression after TBI. We demonstrate different astroglial marker-specific kinetics, paralleling previous observations using an entirely different biomarker panel.[91] Yet, this study's novelty is in the identification of patterns and underlying mechanisms of biomarkers related in their kinetics. The EFA revealed two biomarker groups with differential kinetics that aligned with in vitro release observations; thus, cell injury processes contribute to biomarker fluid kinetics.

Proteolytic degradation also contributes to kinetic differences between biomarkers. ALDOC shows remarkable CSF stability over the first post-injury week and was found to be elevated simultaneously in blood of TBI patients. ALDOC serum levels are reported to be stable up to three weeks in sheep and bovine blood, but decrease over 28 days after controlled cortical contusion in rat.[47,92,93] ALDOC proteolysis by calpain or cathepsin produces a 38 kD ALDOC fragment on later post-injury days.[94–96] In contrast, GFAP proteolysis by calpains or caspases produces massive enzymatic degradation into several fragments that are reported in CSF from patients with various neurodegenerative diseases.[97–101] Thus, our data show that protein-specific breakdown contributes to different temporal biomarker profiles. BLBP and PEA15 levels were highly variable, likely reflecting their very short biofluid stability, yet they are also found on later post-injury days.[102] Hence, these small-sized markers are suited to capture injury progression and secondary adverse events. Overall, our data document diversity in the kinetics of astroglial biomarker patterns caused by differences in release and degradation.

Proteins such as GFAP may pass from CSF to blood via overnight glia-mediated CSF clearance as recently reported.[103] Yet, hyper-acute blood presence of AID markers suggests immediate release after a traumatic impact and direct passage into the circulation. Astrocytes are gatekeepers in the neuro-vascular unit: perivascular astrocytes are part of the blood–brain diffusion barrier (BBB) and astroglial endfeet cover microvessels nearly completely.[104,105] ALDOC is present in astroglial process endings and could be directly released with their rupture.[30] TBI disrupts the microvasculature and damages astroglial fibers, resulting in BBB permeability.[13,24,68,106,107] This makes the presence of ALDOC and other cytosolic AID markers in blood plausible. Interestingly, BBB disruption is also documented in the early hours after mild TBI from mild cortical fluid percussion and blast shock waves.[108,109] Additionally, neocortical BBB permeability is documented in mild TBI patients.[110] Finally, blood elevation of astroglial marker S100 β indicates BBB permeability, and occurs after mild TBI and/or repeated sub-concussive events.[111,112] Hence, cytosolic astroglial proteins, including ALDOC, BLBP and PEA15, are situated for fast release and direct passage into circulation, even after mild mechanical impacts.

AID biomarker panel uniqueness and significance for future TBI patient assessment and monitoring

Confounding variables of age and gender were matched in this study, while medications and comorbidities were not controlled for. The retrospective clinical studies were limited in cohort size, and as such, provide introductory evidence for AID marker elevation and profiles in TBI patients. Our new data on ALDOC, BLBP and PEA15 kinetics after mild TBI differ from those of GFAP and similar cytoskeletal and associated proteins; validation studies for AID biomarkers on larger cohorts are needed. Methodological rigor is provided by using two technically independent assays to validate biomarker measurements. Data analysis was separated by day. Given the short-lived nature of some biomarkers, future finer-resolution kinetic studies are advised.

Selection of unique biomarkers was achieved using astrocyte enrichment and trauma-release. All markers are highly enriched in the CNS: ALDOC is among the most abundant of brain proteins[45,113] and BLBP, GS and PEA15 are expressed highest in the CNS. Thus, the combined biofluid elevation of any two astrocyte-

enriched biomarkers presented here points exclusively and sensitively to CNS injury.

A biomarker panel is anticipated to improve TBI patient assessment compared to a single marker.[114] Several neurotrauma biomarkers have been previously combined to evaluate patients with CNS injuries.[16,91,115] Unsupervised factor analysis is typically used for psychological scores aiding in cognitive assessment of TBI patients.[116,117] To our knowledge, this is the first study to apply EFA on a new small neurotrauma biomarker panel that revealed kinetic differences. Surprisingly, clinical biomarker groups aligned with those generated by the culture trauma model, emphasizing the importance of analyzing biomarker profiles in both clinical and model biofluids after trauma. Aldolases, among other enzymes, have been analyzed before in biofluids of patients with brain injuries, but isoforms were not distinguished.[118] ALDOC, which was evaluated after cerebrovascular disease and other neurological disorders, is identified in a rat cortical contusion and hypoxia model but has not been quantified in human TBI.[47,119,120] BLBP and its heart-specific isoform have been considered as brain injury markers.[102]

This study uniquely links cellular injury stages with biomarker release and delivers clinically relevant fluid biosignatures of brain trauma. Aligning with clinical findings, in vitro data confirm AID marker elevation after mild trauma and differential cellular and clinical release kinetics between biomarkers. Taken together, our data inform on underlying cellular injury processes and introduce AID biomarkers as future tools for neurotrauma assessment.

Funding

The author(s) disclosed receipt of the following financial support for the research, authorship, and/or publication of this article: This work was supported by NIH/NINDS R21NS072606-01A1, the Nick Buoniconti Fund in Miami, The Brain Injury Research Center (BIRC) at UCLA and Abbott Diagnostics.

Acknowledgements

We very much appreciate the extensive input and guidance of statistician Jeff Gornbein, UCLA Department of Biomathematics, SBCC. We are very thankful to Gerry Shaw (EnCor Inc) for providing various antibodies and pure proteins, Lysann Fey and Ingo Curdt (Abbott Diagnostics) for providing input and proteins. We thank UCLA students for their help with data analysis (David Sanville, Akshay Ravi, Rita Bedrossian, Matthew Ji) and Melania Apostolidou for her assistance with experiments. Denise Gellene (CNSI at UCLA) provided language input. Melissa Sondej (Molecular Instrumentation Center, MIC at UCLA) and Cuiwen He (UCLA Department of Chemistry and Biochemistry) provided additional technical assistance. We appreciate the support from Anne Fagan for providing control CSF and blood samples (Alzheimer Disease Research Center, ADRC, Univ. Washington). We thank IDDRC directors Susan Bookheimer and Jean de Vellis for support and for providing cell culture facilities. We acknowledge Zsuzsanna Nemeth, Jessie Truettner (University of Miami), Matthew McFarlane, Stephanie Wolahan and Alyson Thien (Brain Injury Research Center, BIRC at UCLA) for their help with sample selection, shipment and clinical data. Thanks for relevant input from Claude Ruffalo and Michael Sofroniew (Dept Neurobiology at UCLA).

Declaration of conflicting interests

The author(s) declared the following potential conflicts of interest with respect to the research, authorship, and/or publication of this article: Drs. Wanner and Loo have a pending International Patent Application: ''Astrocyte traumatome and neurotrauma biomarkers'' PCT/US16/31043. 5 May 2016; published 10 November 2016.

Author's contributions

IBW, JH, KI, JL conducted experiments and assembled data and figures. GC designed and conducted multiple reaction monitoring (MRM-MS) and analytical mass spectrometry (MS) studies. SS conducted MRM-MS and analytical MS studies, analyzed and assembled data and figures and contributed to the manuscript. IBW and JH wrote the manuscript. JH, ACC, JL and IBW analyzed data and edited the entire manuscript. IBW and JAL conceived the concept and designed the study. JAL supervised all MS studies, advised on protein biochemistry and edited the manuscript. DD, PV and DH provided input on TBI pathophysiology and edited the manuscript. DD, RB, PV, TG and SM provided TBI patient biofluid samples, advised on clinical data and provided editorial input to the manuscript.

Supplementary material

Supplementary material for this paper can be found at the journal website: http://journals.sagepub.com/home/jcb

Supplementary Materials and Methods

Figure S1: Immunoblot measurement
Tables 1: Clinical information and experimental replicates of 1(A): Control subjects; 1(B): Severe and moderate TBI patients and 1(C): Mild TBI patients.
Table 2: List of primary antibodies with epitopes.
Table 3: List of pure proteins.
Table 4: List of secondary antibodies.
Table 5: List of MRM-MS, peptides and ion transitions.

Supplementary Figures

Figure S2: Venn diagram of TBI and Control CSF proteomes.
Figure S3: Flow chart illustrating approach
Figure S4: PTGDS and small GFAP-BDP CSF levels in TBI survivors and nonsurvivors.
Figure S5: BLBP and GFAP are co-expressed in human astrocytes.

Supplementary Tables

Table 6: TBI patients and control subjects CSF proteomes.
Table 7: Biomarker panel Spearman correlations in TBI patients.

References

1. Roozenbeek B, Maas AI and Menon DK. Changing patterns in the epidemiology of traumatic brain injury. *Nat Rev Neurol* 2013; 9: 231–236.
2. Rosenbaum SB and Lipton ML. Embracing chaos: the scope and importance of clinical and pathological heterogeneity in mTBI. *Brain Imag Behav* 2012; 6: 255–282.
3. Buki A, Kovacs N, Czeiter E, et al. Minor and repetitive head injury. *Adv Tech Stand Neurosurg* 2015; 42: 147–192.
4. Helmick KM, Spells CA, Malik SZ, et al. Traumatic brain injury in the US military: epidemiology and key clinical and research programs. *Brain Imag Behav* 2015; 9: 358–366.
5. Montenigro PH, Alosco ML, Martin BM, et al. Cumulative head impact exposure predicts later-life depression, apathy, executive dysfunction, and cognitive impairment in former high school and college football players. *J Neurotrauma* 2016; 34: 328–340.
6. Brogan ME and Provencio JJ. Spectrum of catastrophic brain injury: coma and related disorders of consciousness. *J Crit Care* 2014; 29: 679–682.
7. Mushkudiani NA, Hukkelhoven CW, Hernandez AV, et al. A systematic review finds methodological improvements necessary for prognostic models in determining traumatic brain injury outcomes. *J Clin Epidemiol* 2008; 61: 331–343.
8. Bergsneider M, Hovda DA, Lee SM, et al. Dissociation of cerebral glucose metabolism and level of consciousness during the period of metabolic depression following human traumatic brain injury. *J Neurotrauma* 2000; 17: 389–401.
9. Meier TB, Bellgowan PS, Singh R, et al. Recovery of cerebral blood flow following sports-related concussion. *JAMA Neurol* 2015; 72: 530–538.
10. Farkas O, Lifshitz J and Povlishock JT. Mechanoporation induced by diffuse traumatic brain injury: an irreversible or reversible response to injury? *JNeurosci* 2006; 26: 3130–3140.
11. Barbee KA. Mechanical cell injury. *Ann N Y Acad Sci* 2005; 1066: 67–84.
12. Povlishock JT and Pettus EH. Traumatically induced axonal damage: evidence for enduring changes in axolemmal permeability with associated cytoskeletal change. *Acta Neurochir Suppl* 1996; 66: 81–86.
13. Colombo JA, Yanez A and Lipina SJ. Interlaminar astroglial processes in the cerebral cortex of non human primates: response to injury. *J Hirnforsch* 1997; 38: 503–512.
14. Buki A, Siman R, Trojanowski JQ, et al. The role of calpain-mediated spectrin proteolysis in traumatically induced axonal injury. *J Neuropathol Exp Neurol* 1999; 58: 365–375.
15. Lubieniecka JM, Streijger F, Lee JH, et al. Biomarkers for severity of spinal cord injury in the cerebrospinal fluid of rats. *PloS One* 2011; 6: e19247.
16. Buonora JE, Yarnell AM, Lazarus RC, et al. Multivariate analysis of traumatic brain injury: development of an assessment score. *Front Neurol* 2015; 6: 68.
17. Dash PK, Zhao J, Hergenroeder G, et al. Biomarkers for the diagnosis, prognosis, and evaluation of treatment efficacy for traumatic brain injury. *Neurotherapeutics* 2010; 7: 100–114.
18. Chou SH and Robertson CS, Participants in the International Multi-disciplinary Consensus Conference on the Multimodality M. Monitoring biomarkers of cellular injury and death in acute brain injury. *Neurocrit Care* 2014; (21 Suppl 2): S187–S214.
19. Boutte AM, Yao C, Kobeissy F, et al. Proteomic analysis and brain-specific systems biology in a rodent model of penetrating ballistic-like brain injury. *Electrophoresis* 2012; 33: 3693–3704.
20. Agoston DV. Of Timescales, animal models, and human disease: the 50th anniversary of C. elegans as a biological model. *Front Neurol* 2013; 4: 129.
21. Sjodin MO, Bergquist J and Wetterhall M. Mining ventricular cerebrospinal fluid from patients with traumatic brain injury using hexapeptide ligand libraries to search for trauma biomarkers. *J Chromatograph B Analyt Technol Biomed Life Sci* 2010; 878: 2003–2012.
22. Hanrieder J, Wetterhall M, Enblad P, et al. Temporally resolved differential proteomic analysis of human ventricular CSF for monitoring traumatic brain injury biomarker candidates. *J Neurosci Meth* 2009; 177: 469–478.
23. Poste G. Biospecimens, biomarkers, and burgeoning data: the imperative for more rigorous research standards. *Trends Mol Med* 2012; 18: 717–722.
24. Muoio V, Persson PB and Sendeski MM. The neurovascular unit – concept review. *Acta Physiol* 2014; 210: 790–798.
25. Magistretti PJ. Neuron-glia metabolic coupling and plasticity. *Exp Physiol* 2011; 96: 407–410.
26. Lovatt D, Sonnewald U, Waagepetersen HS, et al. The transcriptome and metabolic gene signature of protoplasmic astrocytes in the adult murine cortex. *J Neurosci* 2007; 27: 12255–12266.
27. Pelvig DP, Pakkenberg H, Stark AK, et al. Neocortical glial cell numbers in human brains. *Neurobiol Aging* 2008; 29: 1754–1762.
28. Wanner IB, Anderson MA, Song B, et al. Glial scar borders are formed by newly proliferated, elongated astrocytes that interact to corral inflammatory and fibrotic cells via STAT3-dependent mechanisms after spinal cord injury. *J Neurosci* 2013; 33: 12870–12886.
29. Li DR, Ishikawa T, Quan L, et al. Morphological analysis of astrocytes in the hippocampus in mechanical asphyxiation. *Leg Med* 2010; 12: 63–67.
30. Levine J, Kwon E, Sondej M, et al. Traumatically injured astrocytes release a proteomic signature modulated by STAT3 dependent cell survival. *Glia* 2016; 64: 668–694.
31. Cahoy JD, Emery B, Kaushal A, et al. A transcriptome database for astrocytes, neurons, and oligodendrocytes: a new resource for understanding brain development and function. *J Neurosci* 2008; 28: 264–278.

32. Sondej M, Doran P, Loo JA, et al. Sample preparation of primary astrocyte cellular and released proteins for 2-D gel electrophoresis and protein identification by mass spectrometry. In: Ivanov A and Lazarev A (eds) *Sample preparation in biological mass spectrometry*. Dordrecht: Springer, 2011, pp.829–849.
33. Protection of human subjects; Belmont Report: notice of report for public comment. *Fed Regist* 1979; 44: 23191–23197.
34. Manley GT, Diaz-Arrastia R, Brophy M, et al. Common data elements for traumatic brain injury: recommendations from the biospecimens and biomarkers working group. *Arch Phys Med Rehab* 2010; 91: 1667–1672.
35. Wanner IB. An in vitro trauma model to study rodent and human astrocyte reactivity. *Meth Mol Biol* 2012; 814: 189–219.
36. Wanner IB, Deik M, Torres M, et al. A new in vitro model of the glial scar inhibits axon growth. *Glia* 2008; 56: 1691–1709.
37. Fabrigar LR and Wegener DT. *Exploratory factor analysis*. Oxford; New York: Oxford University Press, 2012, p.viii, 159 p.
38. Harmon HH. *Modern factor analysis*. Chicago: University of Chicago Press, 1976.
39. Breiman L. *Classification and regression trees*. Belmont, CA: Wadsworth International Group, 1984, p.x, 358 p.
40. Crowder MJ and Hand DJ. *Analysis of repeated measures*. *Monographs on statistics and applied probability*. 1st ed. London/New York: Chapman and Hall, 1990, pp.1–59.
41. Omenn GS, States DJ, Adamski M, et al. Overview of the HUPO plasma proteome project: results from the pilot phase with 35 collaborating laboratories and multiple analytical groups, generating a core dataset of 3020 proteins and a publicly-available database. *Proteomics* 2005; 5: 3226–3245.
42. Bekar L, Libionka W, Tian GF, et al. Adenosine is crucial for deep brain stimulation-mediated attenuation of tremor. *Nat Med* 2008; 14: 75–80.
43. Schenk S, Schoenhals GJ, de Souza G, et al. A high confidence, manually validated human blood plasma protein reference set. *BMC Med Genom* 2008; 1: 41.
44. Kapushesky M, Adamusiak T, Burdett T, et al. Gene Expression Atlas update – a value-added database of microarray and sequencing-based functional genomics experiments. *Nucl Acids Res* 2012; 40: D1077–D1081.
45. Haimoto H and Kato K. Highly sensitive enzyme-immunoassay for human-brain aldolase-C. *Clin Chim Acta* 1986; 154: 203–212.
46. Devoto C, Arcurio L, Fetta J, et al. Inflammation relates to chronic behavioral and neurological symptoms in military with traumatic brain injuries. *Cell Trans*. Epub ahead of print 12 October 2016. DOI: 10.3727/096368916X693455.
47. Thelin EP, Just D, Frostell A, et al. Protein profiling in serum after traumatic brain injury in rats reveals potential injury markers. *Behav Brain Res*. Epub ahead of print 31 August 2016. DOI: 10.1016/j.bbr.2016.08.058.
48. Posti JP, Hossain I, Takala RS, et al. Glial fibrillary acidic protein and ubiquitin C-terminal hydrolase-L1 are not specific biomarkers for mild CT-negative traumatic brain injury. *J Neurotrauma* 2017; 34: 1427–1438.
49. Ellis EF, McKinney JS, Willoughby KA, et al. A new model for rapid stretch-induced injury of cells in culture: characterization of the model using astrocytes. *J Neurotrauma* 1995; 12: 325–339.
50. Hinkle DA, Baldwin SA, Scheff SW, et al. GFAP and S100beta expression in the cortex and hippocampus in response to mild cortical contusion. *J Neurotrauma* 1997; 14: 729–738.
51. Pelinka LE, Kroepfl A, Leixnering M, et al. GFAP versus S100B in serum after traumatic brain injury: relationship to brain damage and outcome. *J Neurotrauma* 2004; 21: 1553–1561.
52. Papa L, Brophy GM, Welch RD, et al. Time course and diagnostic accuracy of glial and neuronal blood biomarkers GFAP and UCH-L1 in a large cohort of trauma patients with and without mild traumatic brain injury. *JAMA Neurol* 2016; 73: 551–560.
53. McCrory P, Meeuwisse WH, Aubry M, et al. Consensus statement on concussion in sport: the 4th international conference on concussion in sport held in Zurich, November 2012. *Br J Sports Med* 2013; 47: 250–258.
54. Zetterberg H and Blennow K. Fluid biomarkers for mild traumatic brain injury and related conditions. *Nat Rev Neurol* 2016; 12: 563–574.
55. Boutte AM, Deng-Bryant Y, Johnson D, et al. Serum glial fibrillary acidic protein predicts tissue glial fibrillary acidic protein break-down products and therapeutic efficacy after penetrating ballistic-like brain injury. *J Neurotrauma* 2016; 33: 147–156.
56. Mondello S, Shear DA, Bramlett HM, et al. Insight into pre-clinical models of traumatic brain injury using circulating brain damage biomarkers: operation brain trauma therapy. *J Neurotrauma* 2016; 33: 595–605.
57. Zoltewicz JS, Mondello S, Yang B, et al. Biomarkers track damage after graded injury severity in a rat model of penetrating brain injury. *J Neurotrauma* 2013; 30: 1161–1169.
58. Whalen MJ, Dalkara T, You Z, et al. Acute plasmalemma permeability and protracted clearance of injured cells after controlled cortical impact in mice. *J Cereb Blood Flow Metab* 2008; 28: 490–505.
59. Carr W, Yarnell AM, Ong R, et al. Ubiquitin carboxy-terminal hydrolase-l1 as a serum neurotrauma biomarker for exposure to occupational low-level blast. *Front Neurol* 2015; 6: 49.
60. Plog BA and Nedergaard M. Why have we not yet developed a simple blood test for TBI? *Exp Rev Neurother* 2015; 15: 465–468.
61. Lizhnyak PN and Ottens AK. Proteomics: in pursuit of effective traumatic brain injury therapeutics. *Exp Rev Proteom* 2015; 12: 75–82.
62. Latterich M and Schnitzer JE. Streamlining biomarker discovery. *Nat Biotechnol* 2011; 29: 600–602.
63. Strathmann FG, Schulte S, Goerl K, et al. Blood-based biomarkers for traumatic brain injury: Evaluation of research approaches, available methods and potential utility from the clinician and clinical laboratory perspectives. *Clin Biochem* 2014; 47: 876–888.

64. Addona TA, Shi X, Keshishian H, et al. A pipeline that integrates the discovery and verification of plasma protein biomarkers reveals candidate markers for cardiovascular disease. *Nat Biotech* 2011; 29: 635–643.
65. Lee YB, Du S, Rhim H, et al. Rapid increase in immunoreactivity to GFAP in astrocytes in vitro induced by acidic pH is mediated by calcium influx and calpain I. *Brain Res* 2000; 864: 220–229.
66. Du S, Rubin A, Klepper S, et al. Calcium influx and activation of calpain I mediate acute reactive gliosis in injured spinal cord. *Exp Neurol* 1999; 157: 96–105.
67. White RE, McTigue DM and Jakeman LB. Regional heterogeneity in astrocyte responses following contusive spinal cord injury in mice. *J Comp Neurol* 2010; 518: 1370–1390.
68. Sword J, Masuda T, Croom D, et al. Evolution of neuronal and astroglial disruption in the peri-contusional cortex of mice revealed by in vivo two-photon imaging. *Brain* 2013; 136: 1446–1461.
69. Kirov II, Tal A, Babb JS, et al. Proton MR spectroscopy correlates diffuse axonal abnormalities with post-concussive symptoms in mild traumatic brain injury. *J Neurotrauma* 2013; 30: 1200–1204.
70. Lafrenaye AD, McGinn MJ and Povlishock JT. Increased intracranial pressure after diffuse traumatic brain injury exacerbates neuronal somatic membrane poration but not axonal injury: evidence for primary intracranial pressure-induced neuronal perturbation. *J Cereb Blood Flow Metab* 2012; 32: 1919–1932.
71. Sakai K, Fukuda T and Iwadate K. Beading of the astrocytic processes (clasmatodendrosis) following head trauma is associated with protein degradation pathways. *Brain injury* 2013; 27: 1692–1697.
72. Colombo JA, Gayol S, Yanez A, et al. Immunocytochemical and electron microscope observations on astroglial interlaminar processes in the primate neocortex. *J Neurosci Res* 1997; 48: 352–357.
73. Gerstner JR, Vanderheyden WM, LaVaute T, et al. Time of day regulates subcellular trafficking, tripartite synaptic localization, and polyadenylation of the astrocytic Fabp7 mRNA. *J Neurosci* 2012; 32: 1383–1394.
74. Schousboe A, Scafidi S, Bak LK, et al. Glutamate metabolism in the brain focusing on astrocytes. *Adv Neurobiol* 2014; 11: 13–30.
75. Mamczur P, Borsuk B, Paszko J, et al. Astrocyte-neuron crosstalk regulates the expression and subcellular localization of carbohydrate metabolism enzymes. *Glia* 2015; 63: 328–340.
76. Eckert A, Bock BC, Tagscherer KE, et al. The PEA-15/PED protein protects glioblastoma cells from glucose deprivation-induced apoptosis via the ERK/MAP kinase pathway. *Oncogene* 2008; 27: 1155–1166.
77. Mergenthaler P, Kahl A, Kamitz A, et al. Mitochondrial hexokinase II (HKII) and phosphoprotein enriched in astrocytes (PEA15) form a molecular switch governing cellular fate depending on the metabolic state. *Proc Natl Acad Sci U S A* 2012; 109: 1518–1523.
78. Magistretti PJ. Neuron-glia metabolic coupling and plasticity. *J Exp Biol* 2006; 209: 2304–2311.
79. Vespa P, Bergsneider M, Hattori N, et al. Metabolic crisis without brain ischemia is common after traumatic brain injury: a combined microdialysis and positron emission tomography study. *J Cereb Blood Flow Metab* 2005; 25: 763–774.
80. Bergsneider M, Hovda DA, McArthur DL, et al. Metabolic recovery following human traumatic brain injury based on FDG-PET: time course and relationship to neurological disability. *J Head Trauma Rehab* 2001; 16: 135–148.
81. Bartnik BL, Lee SM, Hovda DA, et al. The fate of glucose during the period of decreased metabolism after fluid percussion injury: a 13C NMR study. *J Neurotrauma* 2007; 24: 1079–1092.
82. Hovda DA, Yoshino A, Kawamata T, et al. Diffuse prolonged depression of cerebral oxidative metabolism following concussive brain injury in the rat: a cytochrome oxidase histochemistry study. *Brain Res* 1991; 567: 1–10.
83. Bartnik-Olson BL, Oyoyo U, Hovda DA, et al. Astrocyte oxidative metabolism and metabolite trafficking after fluid percussion brain injury in adult rats. *J Neurotrauma* 2010; 27: 2191–2202.
84. Bullock R, Maxwell WL, Graham DI, et al. Glial swelling following human cerebral contusion: an ultrastructural study. *J Neurol Neurosurg Psychiatr* 1991; 54: 427–434.
85. Sutton RL, Hovda DA, Adelson PD, et al. Metabolic changes following cortical contusion: relationships to edema and morphological changes. *Acta Neurochir Suppl* 1994; 60: 446–448.
86. Zhao X, Ahram A, Berman RF, et al. Early loss of astrocytes after experimental traumatic brain injury. *Glia* 2003; 44: 140–152.
87. Lytle JM and Wrathall JR. Glial cell loss, proliferation and replacement in the contused murine spinal cord. *Eur J Neurosci* 2007; 25: 1711–1724.
88. Li DR, Zhang F, Wang Y, et al. Quantitative analysis of GFAP- and S100 protein-immunopositive astrocytes to investigate the severity of traumatic brain injury. *Leg Med* 2012; 14: 84–92.
89. Di Pietro V, Amorini AM, Lazzarino G, et al. S100B and glial fibrillary acidic protein as indexes to monitor damage severity in an in vitro model of traumatic brain injury. *Neurochem Res* 2015; 40: 991–999.
90. Mondello S, Robicsek SA, Gabrielli A, et al. αII-Spectrin breakdown products (SBDPs): diagnosis and outcome in severe traumatic brain injury patients. *J Neurotrauma* 2010; 27: 1203–1213.
91. Papa L, Robertson CS, Wang KK, et al. Biomarkers improve clinical outcome predictors of mortality following non-penetrating severe traumatic brain injury. *Neurocrit Care* 2015; 22: 52–64.
92. Jones DG. Stability and storage characteristics of enzymes in sheep blood. *Res Veterinary Sci* 1985; 38: 307–311.
93. Jones DG. Stability and storage characteristics of enzymes in cattle blood. *Res Veterinary Sci* 1985; 38: 301–306.
94. Pontremoli S, Melloni E, Michetti M, et al. Limited proteolysis of liver aldolase and fructose 1,6-bisphosphatase

by lysosomal proteinases: effect on complex formation. *Proc Natl Acad Sci U S A* 1982; 79: 2451–2454.
95. Offermann MK, Chlebowski JF and Bond JS. Action of cathepsin D on fructose-1,6-bisphosphate aldolase. *Biochem J* 1983; 211: 529–534.
96. Hopgood MF, Knowles SE and Ballard FJ. Proteolysis of N-ethylmaleimide-modified aldolase loaded into erythrocyte ghosts: prevention by inhibitors of calpain. *Biochem J* 1989; 259: 237–242.
97. Zoltewicz JS, Scharf D, Yang B, et al. Characterization of antibodies that detect human GFAP after traumatic brain injury. *Biomark Insights* 2012; 7: 71–79.
98. Fujita K, Kato T, Yamauchi M, et al. Increases in fragmented glial fibrillary acidic protein levels in the spinal cords of patients with amyotrophic lateral sclerosis. *Neurochem Res* 1998; 23: 169–174.
99. Martinez A, Carmona M, Portero-Otin M, et al. Type-dependent oxidative damage in frontotemporal lobar degeneration: cortical astrocytes are targets of oxidative damage. *J Neuropathol Exp Neurol* 2008; 67: 1122–1136.
100. Mouser PE, Head E, Ha KH, et al. Caspase-mediated cleavage of glial fibrillary acidic protein within degenerating astrocytes of the Alzheimer's disease brain. *Am J Pathol* 2006; 168: 936–946.
101. Chen MH, Hagemann TL, Quinlan RA, et al. Caspase cleavage of GFAP produces an assembly-compromised proteolytic fragment that promotes filament aggregation. *ASN Neuro* 2013; 5: e00125.
102. Pelsers MM, Hanhoff T, Van der Voort D, et al. Brain- and heart-type fatty acid-binding proteins in the brain: tissue distribution and clinical utility. *Clin Chem* 2004; 50: 1568–1575.
103. Plog BA, Dashnaw ML, Hitomi E, et al. Biomarkers of traumatic injury are transported from brain to blood via the glymphatic system. *J Neurosci* 2015; 35: 518–526.
104. Mathiisen TM, Lehre KP, Danbolt NC, et al. The perivascular astroglial sheath provides a complete covering of the brain microvessels: an electron microscopic 3D reconstruction. *Glia* 2010; 58: 1094–1103.
105. Nuriya M, Shinotsuka T and Yasui M. Diffusion properties of molecules at the blood-brain interface: potential contributions of astrocyte endfeet to diffusion barrier functions. *Cereb Cortex* 2013; 23: 2118–2126.
106. Logsdon AF, Lucke-Wold BP, Turner RC, et al. Role of microvascular disruption in brain damage from traumatic brain injury. *Comp Physiol* 2015; 5: 1147–1160.
107. Willis CL, Nolan CC, Reith SN, et al. Focal astrocyte loss is followed by microvascular damage, with subsequent repair of the blood-brain barrier in the apparent absence of direct astrocytic contact. *Glia* 2004; 45: 325–337.
108. Hicks RR, Smith DH, Lowenstein DH, et al. Mild experimental brain injury in the rat induces cognitive deficits associated with regional neuronal loss in the hippocampus. *J Neurotrauma* 1993; 10: 405–414.
109. Shetty AK, Mishra V, Kodali M, et al. Blood brain barrier dysfunction and delayed neurological deficits in mild traumatic brain injury induced by blast shock waves. *Front Cell Neurosci* 2014; 8: 232.
110. Korn A, Golan H, Melamed I, et al. Focal cortical dysfunction and blood-brain barrier disruption in patients with Postconcussion syndrome. *J Clin Neurophysiol* 2005; 22: 1–9.
111. Vajtr D, Benada O, Kukacka J, et al. Correlation of ultrastructural changes of endothelial cells and astrocytes occurring during blood brain barrier damage after traumatic brain injury with biochemical markers of BBB leakage and inflammatory response. *Physiol ResAcadSci Bohemoslov* 2009; 58: 263–268.
112. Marchi N, Bazarian JJ, Puvenna V, et al. Consequences of repeated blood-brain barrier disruption in football players. *PloS One* 2013; 8: e56805.
113. Willson VJ and Thompson RJ. Human brain aldolase C4 isoenzyme: purification, radioimmunoassay, and distribution in human tissues. *Ann Clin Biochem* 1980; 17: 114–121.
114. Silverberg ND, Gardner AJ, Brubacher JR, et al. Systematic review of multivariable prognostic models for mild traumatic brain injury. *J Neurotrauma* 2015; 32: 517–526.
115. Kwon BK, Streijger F, Fallah N, et al. Cerebrospinal fluid biomarkers to stratify injury severity and predict outcome in human traumatic spinal cord injury. *J Neurotrauma* 2016; 34: 567–580.
116. Bohac DL, Malec JF and Moessner AM. Factor analysis of the mayo-portland adaptability inventory: structure and validity. *Brain Injury* 1997; 11: 469–482.
117. DeJong J and Donders J. A confirmatory factor analysis of the California Verbal Learning Test–Second Edition (CVLT-II) in a traumatic brain injury sample. *Assessment* 2009; 16: 328–336.
118. Klun B. Spinal fluid and blood serum enzyme activity in brain injuries. *J Neurosurg* 1974; 41: 224–228.
119. Asaka M, Kimura T, Nishikawa S, et al. Serum aldolase isozyme levels in patients with cerebrovascular diseases. *Am J Med Sci* 1990; 300: 291–295.
120. Willson VJ, Graham JG, McQueen IN, et al. Immunoreactive aldolase C in cerebrospinal fluid of patients with neurological disorders. *Ann Clin Biochem* 1980; 17: 110–113.